Received 8 April 2024; revised 15 May 2024; accepted 26 May 2024. Date of publication 29 May 2024; date of current version 6 August 2024.

Digital Object Identifier 10.1109/OJAP.2024.3407053

Beamforming of Transmit Antennas Using Grey Wolf Optimization and L_2-Norm for Performance Enhancement of Beyond 5G Communications

SAMAR I. FARGHALY[1], MOSTAFA M. FOUDA[2], (Senior Member, IEEE), AND MANAL M. EMARA[3], (Member, IEEE)

[1]Electronics and Electrical Communications Engineering Department, Faculty of Engineering, Tanta University, Tanta 31527, Egypt

[2]Department of Electrical and Computer Engineering, Idaho State University, Pocatello, ID 83209, USA

[3]Department of Electrical Engineering, Faculty of Engineering, Kafrelsheikh University, Kafrelsheikh 33511, Egypt

CORRESPONDING AUTHOR: M. M. FOUDA (e-mail: mfouda@ieee.org)

ABSTRACT Pattern synthesis is widely used in many radar and communication systems and received great interest. So, this paper proposes a new beamforming strategy based on a hybrid combination between grey wolf optimizer (GWO) with L_2-norm called proposed GWO. This approach is applied to synthesized uniform linear arrays (ULA), Chebyshav arrays, and shaped pattern arrays. Moreover, it is utilized for side lobe level (SLL) and size reduction of antenna elements. In this strategy, the GWO is utilized to optimize the element spacing to adjust the half-power beamwidth (HPBW) to save it the same as desired pattern. Furthermore, the excitations of the antenna elements are optimized via the L_2-norm minimization problem. The proposed GWO has low complexity (fewer iterations and computing time) compared to other algorithms. In addition, it has a very accurate approximation of the original radiation pattern. As well, the computer simulation technology (CST) microwave package is utilized to achieve the practical validation of the proposed methodologies. As an application of the proposed GWO, it is employed to create a proposed hybrid beamforming (PHB) structure for Multi-input Multi-output (MIMO) systems. Consequently, the BS transmitting antennas are synthesized for gain maximization while utilizing the current amount of antenna elements. This results in considerable savings in antenna components and associated radio frequency (RF) chains which reduces system complexity. Furthermore, array gain maximization will increase the received signal-to-noise ratio (SNR). In addition, the SLL reduction scenario will decrease the interference from undesired users which in turn will also increase SNR. Hence, the performance of the system in terms of spectral efficiency (SE) and power utilization will be improved.

INDEX TERMS Antenna array synthesis, beamforming, Chebyshev array, grey wolf optimizer, MIMO, side lobe level, uniform linear array.

I. INTRODUCTION

ANTENNAS have long been considered one of the most essential components in wireless communications and fifth-generation (5G) networks [1], [2], [3]. They are utilized extensively in telecommunication, signal processing, radar systems, and many other applications. Due to its benefit of offering high gains and spectrum efficiency, smart antennas have been a trending emphasis for most technologically-based industries in this period of developing a smart world. Additionally, it possesses unique characteristics such as adaptive beamforming and beam steering capabilities [4], [5]. However, improvements in network coverage, capacity, and quality of service are required due to the advancements in wireless communication technology and the increasing number of users.

As a result, significant efforts have been made to investigate array antennas with higher gain, higher directivity, enhanced beam steering (BS) performance, and lower side lobe level

(SLL) [6], [7], [8]. Furthermore, to increase the antenna directivity, the number of antenna elements must be increased.

So, the most efficient algorithms are utilized to reduce the number of antenna elements with maintaining higher gain and directivity [9], [10]. These algorithms are synthesize the antenna patterns where the amplitudes, phases, placements of the excitations, and the interelement spacing are controlled to accomplish array synthesis [11], [12].

A. RELATED WORK

Many practical wireless communication systems need the radiation pattern of the antenna arrays to match certain fundamental parameters, such as the half-power beam width (HPBW) and SLL, to increase directivity, limit user interference during reception, and reduce power consumption during transmission [13], [14], [15], [16], [17], [18], [19], [20]. A variety of antenna array synthesis methods have been presented either for linear antenna arrays (LAA) [3], [9], [21], and [22], circular arrays [23], [24], [25], [26], or cylindrical arrays [27]. The authors in [3] utilized the combination of genetic algorithm (GA) and convex optimization (CVX) called GA/L1 for LAA synthesis to synthesize the LAA. The GA algorithm optimizes the element spacing while convex optimization determines the excitation coefficients via solving the L1 minimization problem to reduce the number of antenna elements while maintaining HPBW. In addition, the hybrid combination between the method of moments (MoM) and the GA in [9] creates different patterns with the fewest possible antenna components. One benefit of using the analytical MoM is that it yields a well-conditioned matrix that can solve the issue without any special treatment. Compared to MOM/GA, GA/L1 [3] achieves less dynamic range ratio (DRR) and the least mean square error (LMSE).

Furthermore, for LAA synthesis, the purpose of the study in [27] is to demonstrate the application of ant colony optimization (ACO), a well-known form of evolutionary computer optimization approach, to the classic electromagnetic issue of linear array synthesis. An algorithm based on the principles of ant colony optimization has been created to achieve this goal. Real numbers are used in the method. A few instances utilizing various optimization standards are demonstrated. Additionally, some instructions are provided on how to utilize the technique, particularly for generating the desirability function. It has been shown that the approach is adaptable and practical for this particular situation. The work aims to demonstrate (through this specific application) the adaptability and simplicity of this algorithm family, which renders it appropriate for application in various electromagnetic optimization situations.

In [28], a sector beam pattern and a null-controlled pattern are designed using Taguchi's method, a novel approach to global electromagnetic optimization. An extensive implementation process is provided. This work demonstrates how the suggested approach may quickly converge on the best designs and simplicity to use. As mentioned before, SLL reduction play an important role in interference suppression in communication systems. In this regard, the papers [13], [15], [17], [29]–[35] are interested in performing different algorithms for SLL reduction.

A Mayfly (MA)-based optimization technique performed by the authors in [13] for the pattern synthesis of 10, 16, 20, and 32 components LAA is presented in this study. Four optimization challenges were created and MA was used to solve them to investigate the capabilities of MA. The results of this algorithm show that the performance of the MA outperformed other algorithms on the comparison in reducing SLL. On the other hand, for maximum SLL reduction of the LAA and CAA beam pattern synthesis using invasive weed optimization (IWO) is performed in [15]. To start, the authors in [15] created an optimization problem for the beam pattern that lowers the maximum SLLs of the CAA and LAA. Second, they solved the issue formulation using the IWO algorithm. Subsequently, the IWO algorithm's primary parameters are adjusted to get optimal beam pattern synthesis performance. To confirm the efficacy of IWO, they lastly run simulations for the LAA and CAA using varying numbers of antenna elements. Additionally, electromagnetic simulations are used to assess the beam patterns in real-world circumstances. The outcomes from [15] demonstrate that IWO performs the best for the LAA and CAA optimization issues when compared to other algorithms. Furthermore, the authors in [17] perform the GWO for antenna array optimization. In this work, GWO has been used for optimum pattern synthesis in two ways: first, by optimizing antenna locations under the assumption of uniform excitation, and second, by optimizing antenna current amplitudes under the assumption of uniform array spacing and phase. GWO is used to put deep nulls in the designated directions. Furthermore, GWO is used to manage the other side lobes concurrently and minimize the first side lobe closest to the main beam. This process is known as near-side lobe minimization.

The authors in [29] developed a multi-objective optimization problem (MOP) to concurrently reduce the mission completion time, the overall energy cost of the unmanned aerial vehicles (UAVs), and the signal strength towards the eavesdropper. In [30], the authors demonstrated that the MOP is a large-scale, mixed-variable, NP-hard optimization problem. In order to identify a collection of candidate solutions with multiple trade-offs that can satisfy different requirements in low computational complexity, we thus present a swarm intelligence-based approach. We further demonstrate that, when dealing with mixed-variable optimization and large-scale issues, swarm intelligence approaches must improve the phases of solution initialization, solution update, and algorithm parameter updating. The suggested algorithm works better than cutting-edge swarm intelligence systems, according to simulation data, and it may also greatly save time and energy expenses. Consequently, in order to minimize the maximal SLL, the authors in [30] developed a hybrid discrete and continuous optimization

problem (HDCOP). In order to solve HDCOP, both discrete and continuous issues must be solved concurrently. To this end, we provide distributed CB techniques based on consensus as well as centralized approaches. HDCOP is broken down into two sub-optimization issues for the centralized approach and provides a discrete cuckoo search (CS) technique to optimize the node location selection and a continuous CS algorithm to maximize the excitation current weights of the chosen nodes. Because of SLL reduction and minimizing the number of antennas importance in the wireless communication system as mentioned before, it is applied to the millimeter wave (mmWave) Multiple-input multiple-output (MIMO) technology as an application [36], [37], [38], [39].

MmWave increases the carrier frequency significantly, resulting in a wide range of usable spectrum bands. Moreover, using microstrip technology allows a large number of antenna components to be crammed into a small space since working in the high-frequency region reduces the size of the antenna [40]. The mmWave MIMO system has a high bit error rate and increased system complexity despite achieving enhanced spectral efficiency (SE) and efficient power consumption, particularly when including a large number of data streams or users. In addition, the fully digital precoding in mmWave system is costly and consumes a lot of power [40]. As a result, Hybrid analog/digital beamforming is the optimal approach for overcoming the constraints of pure digital or analog beamforming in both single and multiuser scenarios. The complexity of the system regarding radio frequency chains (RF) can be reduced, in addition, analog phase shifters can be used for the implementation of analog beamforming [41]. The hybrid system has the benefit of digital precoding in the transmitter and a combiner in the receiver, which reduces the precision of residual multi-streams in analog [42]. Previous research provides an overview of hybrid precoding. Authors in [42] proposed a two-step beamforming method for MIMO systems using a Kalman precoder. First, the RF precoding and combining matrix are computed. Then, construct the digital baseband precoder at the BS. The author of [43] suggested a hybrid precoding structure based on switching networks. The authors in [44] suggested hybrid precoding with MMSE and rate fairness among users, [43] provided an algorithm with orthogonal matching pursuit (OMP), [45] highlighted the low complexity of a multiuser hybrid precoding structure using MMSE, and [46] presented a method to increase spectral efficiency and analyze numerical results for spatially sparing mmWave systems.

B. CONTRIBUTION

In this paper, a beamforming approach based on the GWO and L_2-norm is used for LAA synthesis is introduced. The GWO has many significant advantages, such as, simple implementation, quick convergence, and excellent convergence results [10]. In [10], the authors compared between GWO and other algorithms. The results show that the GWO gives better results than other algorithms. So, The GWO is used to optimize the element spacing and L_2-norm minimization problem is used to calculate the excitation coefficients to obtain the optimal solutions. The proposed scheme has two parts. First: Reducing the number of antenna elements which it reduce the needed amount of radio of RF chains in MIMO systems, and this achieves energy efficiency and reduce the complexity of the system. Second: an SLL reduction algorithm is proposed. The benefit of SLL is that it reduces interference and hence it enhances the performance of communication systems. As well, beamforming will lead to a decrease in the most cost-effective and sophisticated circuitry in MIMO systems by a reduction in the number of antenna elements and the needed RF. Based on the synthesized or beamformed array structure using the proposed GWO), a hybrid beamforming structure (PHB) is proposed to improve the SE of MIMO systems. We suggest the use of the proposed GWO beamforming technology to get optimal gain from the BS antenna array while employing a typical LAA.

An overview of the main developments and contributions made by this effort is provided below:

- Introduce the proposed algorithm based on GWO and L_2-norm for reducing the number of antenna elements while maintaining HPBW, SLL, and gain. In addition, the DRR is reduced compared to other algorithms.
- The reduction in the number of antenna elements will reduce complexity and improve energy efficiency in communication systems that meet the demands of beyond 5G. this paper obtain the highest reduction in the antenna elements reached to ($N = 11$)
- Furthermore, the proposed GWO is used for SLL reduction to decrease the interference between users, which enhances communication performance.
- The number of iterations needed to obtain optimal results is less than other algorithms in literature and comparison, so the execution time is less.
- The CST microwave package is utilized to achieve the practical validation of the suggested methodologies using dipole antennas instead of isotropic antennas.
- In addition, as an application of the proposed GWO algorithm. It is employed to create a PHB structure for MIMO systems to maximize gain while utilizing the existing number of antennas. The proposed GWO is employed to fully utilize the transmit array elements in the PHB structure to synthesize the radiation pattern.

The remaining sections of the paper are arranged as follows: Grey Wolf Optimizer (GWO) and problem formulation of the array synthesis is covered in Section II, the proposed GWO array synthesis approach is introduced in Section III, and the simulation results of the proposed GWO technique are shown in Section IV. Section V presents the MIMO system model and theoretical analysis, while Section VI performs the proposed hybrid beamforming

design. Section VII presents the simulation results of PHB algorithms, and finally, Section VIII presents the conclusions.

II. GREY WOLF OPTIMIZER (GWO)

The GWO technique is widely used to solve optimization problems in a variety of fields due to its many significant advantages, which include easy implementation, quick convergence, and excellent convergence results. As a result, the GWO has quickly attracted significant scientific interest and a wide readership in a variety of fields. So it is used to synthesize LAA. In addition, the GWO algorithm is a metaheuristic optimization algorithm inspired by the social hierarchy and hunting behavior of grey wolves. It uses a hierarchical structure and cooperation among individuals to optimize solutions to complex problems. In the GWO algorithm, the grey wolves are divided into four hierarchical levels: alpha, beta, delta, and omega. The alpha wolf is the leader of the pack and has the highest fitness value, while the omega wolf is the weakest and has the lowest fitness value. The hunting behavior of the wolves is simulated to optimize a given problem. To find the optimal solution, the GWO algorithm follows these steps:

- Initialization: The algorithm starts by initializing a population of grey wolves, with each wolf representing a potential solution.
- Objective Function Evaluation: The fitness of each wolf is evaluated by applying the objective function to its position.
- Leader Selection: The wolves with the highest fitness values are selected as leaders.
- Exploration: The leaders explore the search space by updating their positions based on specific equations.
- Prey Selection: The prey is selected based on the fitness values of the wolves and their positions.
- Feeding: The prey is chased and captured by the wolves, and their positions are updated accordingly.
- Update Best Solution: The best solution is updated based on the fitness values of the wolves.
- Termination: The algorithm terminates when a stopping criterion is met, such as reaching a maximum number of iterations or achieving a desired fitness value.

III. PROBLEM FORMULATION

The goal of this work is to use the proposed GWO to synthesize an LAA. This is accomplished by determining the set of optimal element amplitude and position values that result in a radiation pattern with a low peak SLL or a low number of antenna elements. As illustrated in Fig. 1, the array factor of an LAA with N antenna elements arranged uniformly with uniform spacing $d_n,\ n = [1, 2, \ldots, N]$ on the Z-axis, and it may be expressed as:

$$AF_{\mathrm{d}}(\theta) = \sum_{n=1}^{N} a_n e^{(j(n-1)\beta \mathrm{d}\cos(\theta))} \tag{1}$$

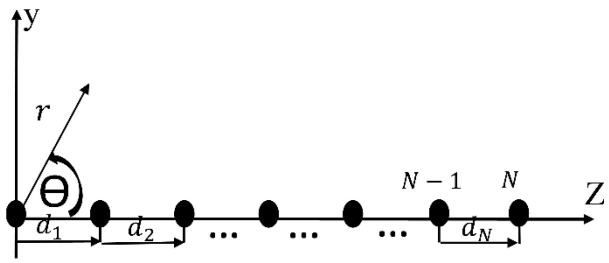

FIGURE 1. Linear antenna array of N elements.

where the original array factor at t observation angles is denoted by $AF_{\mathrm{d}}(\theta) \in \mathbb{C}^{t\times 1}$. a_n is the feeding coefficient of n^{th} element and can be expressed as:

$$a_n = [a_1,\ a_2,\ a_3, \ldots, a_N] \tag{2}$$

$\beta = (2\pi/\lambda)$ is the wave number, and d is the uniform element spacing. Assuming the 1^{st} element is set at $d_1 = d$, so d_n is calculated as:

$$d_n = (n-1)d,\ \ n = 1, 2, \ldots, N \tag{3}$$

Alternatively, a shaped beam LAA with complex current coefficients can be modeled as a shaped beam array. With the least number of elements (N), we want to synthesize the various forms of LAA and produce a synthesized radiation pattern ($AF_{\mathrm{s}}(\theta)$) that closely resembles the original radiation pattern ($AF_{\mathrm{d}}(\theta)$) in the following ways:

$$AF_{\mathrm{s}}(\theta) = AF_{\mathrm{d}}(\theta) \tag{4}$$

where the $AF_{\mathrm{s}}(\theta)$ can be written as:

$$AF_{\mathrm{s}}(\theta) = \sum_{m=1}^{M} a_m \mathrm{e}^{(j(m-1)\beta d_{\mathrm{s}}\cos(\theta))} \tag{5}$$

where a_m denotes the synthesized amplitudes which are expressed as:

$$a_m = [a_1,\ a_2,\ a_3, \ldots, a_M] \tag{6}$$

In addition, d_{s} denotes the synthesized element spacing and the synthesized element position can be expressed as:

$$d_m = (m-1)d_{\mathrm{s}},\ \ m = 1, 2, \ldots, M \tag{7}$$

IV. PROPOSED GWO SYNTHESIS TECHNIQUE

The proposed GWO strategy is based on a hybrid combination between GWO and L_2-norm. The ideal element location d_{s} is determined also by GWO which minimizes the defined cost function. However, L_2-norm is utilized to get the antenna excitation coefficients a_m. Two distinct situations of the optimization issue are examined in this paper. The suggested GWO technique's flow chart is displayed in Fig. 2. We provide the objective functions and design the optimization issue as follows in order to produce an ideal radiation pattern synthesis for LAA by optimizing the excitation currents or inter-element spacing.

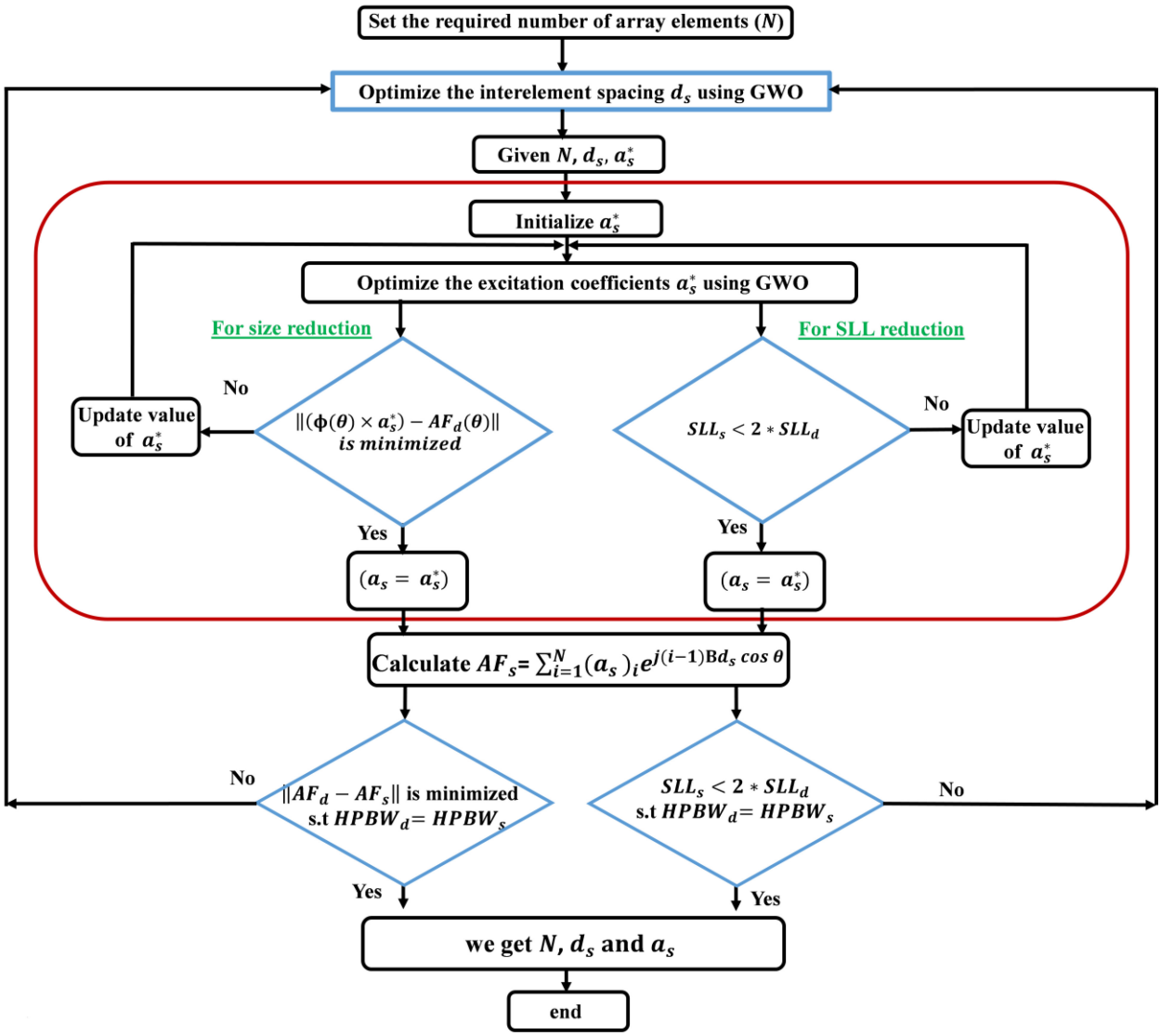

FIGURE 2. Flowchart of the proposed GWO technique for array size and SLL reduction.

A. CASE 1: REDUCTION OF THE NUMBER OF LAA

The array factor model of uniform LAA such as uniform linear array (ULA), Chebyshav array, and shaped arrays are presented in this section. In addition, an objective function is suggested and the optimization issue for several antenna reductions is stated. The steps of the proposed model in Fig. 2 are written as follows:

- Step 1: Determine array elements (N) that are needed to create the original pattern $AF_{\mathrm{d}}(\theta)$.
- Step 2: The synthesized element spacing vector $d_{\mathrm{s}} = [d_{s_1}, d_{\mathrm{s}2}, d_{\mathrm{s}3}, \ldots, d_{\mathrm{s}M}]$ is optimized by the GWO where $0.5\lambda < d_{\mathrm{s}} < 0.9\lambda$.
- Step 3: The synthesized feeding coefficients vector $a_m = [a_1, \ a_2, \ a_3, \ldots, a_M]^T$ is optimized by GWO method [9] and [10].
- Step 4: The GWO method tests and updates the value of the synthesized excitation currents vector a_m via solving the following L_2-norm cost function [10] and [11].

$$\begin{aligned} \mathrm{CF}_1 = \text{minimize} \ & \left\| (\Phi(\theta) \times a_{\mathrm{s}}) - AF_{\mathrm{d}}(\theta) \right\| \\ \text{s.t.} \ & \mathrm{HPBW}_{\mathrm{d}} = \mathrm{HPBW}_{\mathrm{s}} \end{aligned} \tag{8}$$

where $\Phi(\theta) \in C^{t \times N}$ is the direction-finding matrix of the created N-elements array at t observation angles. $HPBW_{\mathrm{d}}$ and $HPBW_{\mathrm{s}}$ are the beam width of the original and synthesized patterns with half powers, respectively.

- Step 5: The synthesized array factor from Eq. (5) is calculated using the estimated excitation coefficient vector a_{s}. The least mean square error (LMSE) between the synthesized and intended patterns in the case of optimization element spacing is then calculated from the defined cost function of the GWO in Eq. (9) if the constraint in Eq. (8) is achieved.

$$\mathrm{CF}_2 = \left(\frac{1}{T} \sum_{t=1}^{T} [|AF_{\mathrm{d}}(t)| - |AF_{\mathrm{s}}(t)|]^2 \right)$$

$$\text{s.t. } \text{HPBW}_\text{d} = \text{HPBW}_\text{s} \tag{9}$$

- Step 6: To update the item's position vector, go back to step 1 and execute steps 2 through 5 once again if the condition $\text{HPBW}_\text{d} = \text{HPBW}_\text{s}$ is not met.
- Step 7: To precisely tune the element spacing vector, go to step 2 and continue steps 2 through 5 till obtaining the least cost function, provided that the criteria $\text{HPBW}_\text{d} = \text{HPBW}_\text{s}$ is met. The optimal vectors for element spacing and element currents are obtained by minimizing the proposed cost function.

B. CASE 2: REDUCTION OF SLL OF ULA

The array factor model of uniform ULA is presented in this section. In addition, an objective function is designed, and the optimization issue for SLL reduction is stated. The steps of the proposed model in Fig. 2 are written as follows:

- Step1: Determine the array elements (N) are needed to create the desired pattern $AF_\text{d}(\theta)$.
- Step 2: The synthesized element spacing vector $d_\text{s} = [d_{s_1}, d_{s2}, d_{s3}, \ldots, d_{sM}]$ is optimized by the GWO, where $0.5\lambda < d_\text{s} < 0.9\lambda$.
- Step 3: The synthesized feeding current vector $a_m = [a_1, \ a_2, \ a_3, \ldots, a_M]^T$ is optimized by GWO method.
- Step 4: The value of synthesized excitation currents vector a_m is tested and updated, via the GWO to solve the following optimization cost function.

$$\begin{aligned} \text{CF}_3 = \text{minimize } & \left(\left\|(\Phi(\theta) \times a_\text{s}) - AF_\text{d}(\theta)\right\|\right) \\ & \text{s.t. } \text{HPBW}_\text{d} = \text{HPBW}_\text{s} \& \ \text{SLL}_\text{s} =< 2 * \text{SLL}_\text{d} \\ & 0.9\lambda \geq d \geq 0.5\lambda \end{aligned} \tag{10}$$

where SLL_d and SLL_s the side lobe are levels of the wanted pattern and created pattern, respectively. They can be calculated as:

$$\text{SLL}_\text{d} = 20 \log_{10} \frac{AF_\text{d}(\theta_{PSL})}{AF_\text{d}(\theta_{ML})} \tag{11}$$

$$\text{SLL}_\text{s} = 20 \log_{10} \frac{AF_\text{s}(\theta_{PSL})}{AF_\text{s}(\theta_{ML})} \tag{12}$$

where $AF_\text{d}(\theta_{ML})$ and $AF_\text{s}(\theta_{ML})$ are the value of the desired and synthesized pattern at the max value of the main lob, respectively. In addition, $AF_\text{d}(\theta_{PSL})$ and $AF_\text{s}(\theta_{\text{PSL}})$ are the values of the desired and synthesized pattern at peak side lobe value, respectively.

- Step 5: Using the estimated excitation coefficient vector a_s, the synthesized array factor from Eq. (5) is computed. If the constraint in Eq. (10) is satisfied, the LMSE between the synthesized and original patterns in the case of the optimization element spacing is then computed using the defined cost function of the GWO in Eq. (13) [10], [11].

$$\text{CF}_4 = \left(\frac{1}{T} \sum_{t=1}^{T} [|AF_\text{d}(t)| - |AF_\text{s}(t)|]^2\right)$$

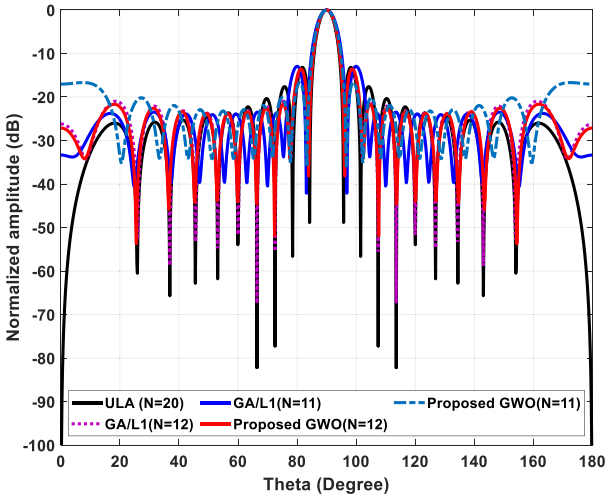

FIGURE 3. Synthesized radiation patterns of proposed GWO with equally spaced 12 and 11 elements against ULA pattern.

$$\text{s.t. } \text{HPBW}_\text{d} = \text{HPBW}_\text{s} \ \& \ \text{SLL}_\text{s} =< 2 * \text{SLL}_\text{d} \tag{13}$$

- Step 6: If the criteria $\text{SLL}_\text{s} =< 2 * \text{SLL}_\text{d}$ and $\text{HPBW}_\text{d} = \text{HPBW}_\text{s}$ are not satisfied, to update the position vector of each element, go back to step 1 and repeat steps 2 through 5.
- Step 7: If the conditions $\text{SLL}_\text{s} =< 2 * \text{SLL}_\text{d}$ and $\text{HPBW}_\text{d} = \text{HPBW}_\text{s}$ are satisfied, go to step 2 and repeat steps 2 through 5 until the cost function is minimized in order to accurately adjust the element spacing vector. By minimizing the suggested cost function, the ideal vectors for d and a_m are obtained.

V. SIMULATION RESULTS OF PROPOSED GWO

In this section, several MATLAB simulations are run to confirm the functioning of the suggested proposed algorithm GWO in reducing SLL and the number of antenna elements of the synthesized ULA. Additionally, the computer simulation technology (CST) microwave studio software package is used to accomplish the practical validation of the suggested methodologies while taking into account a half-wavelength dipole element.

A. REDUCING THE NUMBER OF ANTENNA ELEMENTS

1) PENCIL BEAM ULA

Consider a ULA with $N = 20$ elements placed on the Y-axis with uniform interelement spacing $d = 0.5\lambda$, SLL $= -13.1914$ dB, DRR $= 1$, and the HPBW $= 5.22$. Fig. 3 shows the comparison between the synthesized proposed GWO with $N = 12$, $N = 11$ with ULA, and GA/L1 in [3]. From the results, it is clear that the proposed algorithm with $N = 12$ and interelement spacing $d = 0.85\lambda$ is very close to the original array factor with a 40% reduction in the number of antenna elements. The SLL of the proposed GWO is less than ULA by about 0.5 dB without any change in HPBW.

TABLE 1. Feeding coefficients, *d*, HPBW, SLL, and DRR of the created arrays using the proposed GWO with comparision of the 20-elements ULA.

Algorithm	N	d/λ	Excitation coefficients					SLL (dB)	HPBW	DRR	Gain (dB)	Execution time (s)
ULA	20	0.5	1	1	1	1	1	-13.191	5.22°	1	13.01	0
			1	1	1	1	1					
Proposed GWO	12	0.85	1.3076	1.2618	1.4639	1.6662	1.8001		5.22°	1.47	12.9	5.4
			1.8535	1.8405	1.7765	1.6676	1.5213	-13.579				
			1.3767	1.4015								
Proposed GWO	11	0.897	1.3257	1.2798	1.4188	1.5688	1.6860	-16.684	5.23°			
			1.7500	1.7469	1.6650	1.5002	1.2630			1.8	12.4	3.04
			0.9681									
GA/L1	12	0.833	1.2474	1.3649	1.5852	1.7372	1.7451	-14.195	5.22°	1.41	12.5	12
			1.6757	1.6454	1.6987	1.7669	1.7383					
			1.5684	1.3430								
GA/L1	11	0.81	0.5857	0.1065	0.4018	0.0828	0.0843	-12.581	5.9400	8.36	10	16.8
			0.0971	0.0918	0.0928	0.0785	0.1011					
			0.0812									

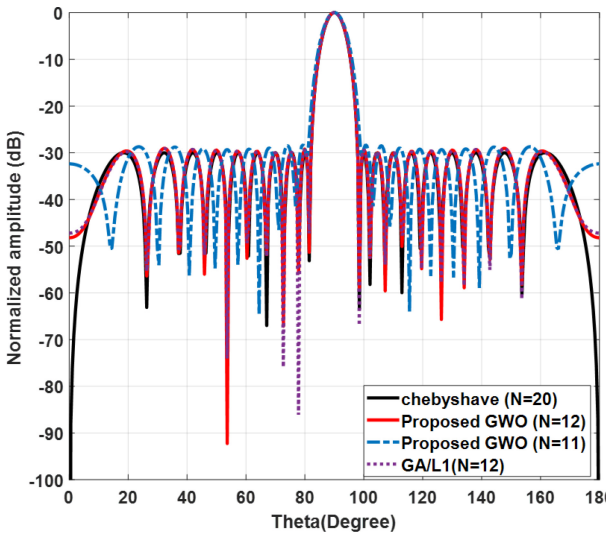

FIGURE 4. Synthesized radiation patterns of proposed GWO with non-equal element spacing against Chebyshev pattern.

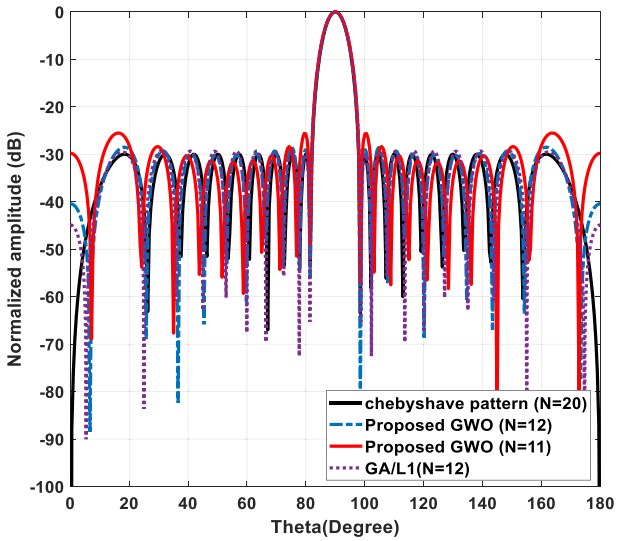

FIGURE 5. Synthesized radiation patterns of proposed GWO with equal element spacing against the Chebyshev pattern.

In addition, for the proposed algorithm with $N = 11$ and $d = 0.897\lambda$, the reduction in antenna elements is 45% with SLL $= -16.68$ dB, while GA/L1 with ($N = 11$) has SLL $= -12.58$ dB and HPBW $= 5.41$ dB. This shows a significant decrease in the SLL as compared to ULA and GA/L1. The HPBW is slightly greater by 0.01° than ULA. The simulation time of the proposed GWO is reduced by 50 % compared to the GA/L1 algorithm [3]. These results confirm that the proposed GWO has better performance than the linear array optimization algorithm called GA/L1. Table 1 summarizes a comparison between synthesized beams against ULA and GA/L1 in terms of excitation coefficients, array gain, DRR, SLL, HPBW, and execution time.

2) PENCIL BEAM CHEBYSCHEV ARRAY

By applying the proposed technique on the Chebyschev array, the results are shown in Fig. 4 for non-equal element spacing and Fig. 5 for equal space. They show a comparison between the Chebyshav array with $N = 20$ and $d = 0.5\ \lambda$ versus the proposed GWO with $N = 11,\ 12$ and GA/L1 [3] with $N = 12$. In Fig. 4, the execution time needed to get the results of the proposed algorithm with $N = 12$ and $N = 11$ is only 5 and 4 seconds, respectively. While GA/L1 needed 30 seconds, which saved 83.3% of the time. The proposed GWO with $N = 12$ is very close to the Chebyshav array which gives the same gain with HPBW = 6.187° and SLL $= -29.999$ dB.

Furthermore, the DRR of the proposed GWO is less than GA/L1. As well, for the proposed GWO with $N = 11$ which gives the same gain $= 16$ dB with the same HPBW of Chebyshav array and SLL $= -28.2113$ dB. The reduction in the number of antenna elements is 45%, which is an excellent result of the synthesized pattern. Furthermore, Fig. 5 for uniform spacing shows that the proposed technique performs well, giving the same HPBW and gain with an acceptable level in SLL. The SLL $= -25.56$ *dB* for the proposed GWO with $N = 11$ and SLL $= -29.9$ *dB* for the proposed GWO with $N = 12$. The execution time to obtain the proposed results is only 4 seconds, while GA/L1 needs 20 seconds. The DRR is better than GA/L1 for $N = 12$.

TABLE 2. Feeding coefficients, d/λ, SLL, HPBW, and DRR of the synthesized arrays for non-uniform spacing poposed GWO and 20-elements Chebyshav array.

Algorithm	N	d/λ	Excitation coefficients				SLL (dB)	HPBW	DRR	Gain (dB)	Execution time (s)
Chebyshav array (N=20)	a_n	1 2.246	0.877 2.552	1.2009 2.802	1.549 2.979	1.905 3.07	-30	6.1879°	3	16.06dB	0
	d/λ	0.5 3	1 3.5	1.5 4	2 4.5	2.5 5					
Proposed GWO (N=12)	a_n	1.3863 5.1867	1.9204	2.9418	3.9449	4.7405	-29.999	6.1879°	3.6	16.08dB	5.83
	d/λ	0.834 5.041	1.667	2.5	3.342	4.19					
Proposed GWO (N=11)	a_n	1.3222 5.244 1.6481	1.8036 5.3014	2.8440 4.7107	3.9323 3.7071	4.8437 2.5639	-28.2113	6.1879°	3.9	16.04dB	4.5
	d/λ	0.84 5.057 9.266	1.668 5.907	2.511 6.753	3.357 7.596	4.207 8.424					
GA/L1 (N=12)	a_n	0 4.2	0.833	1.666	2.5	3.349	-29.99	6.1879°	3.69	16.05	30
	d/λ	1.3984 5.1715	1.9227	2.9390	3.9413	4.7444					

TABLE 3. Excitation coefficients, d/λ, HPBW, SLL, and DRR of the synthesized arrays for uniform spacing proposed GWO and 20-elements Chebyshav array.

Algorithm	N	d/λ	Excitation coefficients					SLL (dB)	HPBW	DRR	Gain (dB)	Execution time (s)
Chebyshav array	20	0.5	1 2.246	0.877 2.552	1.2009 2.802	1.549 2.979	1.905 3.07	-30	6.1879°	3	16.06dB	0
Proposed GWO	12	0.83	1.4172	2.0253	2.9504 5.0769	3.8893	4.6510	-29.9	6.1879°	3.5	16.02dB	4.2
Proposed GWO	11	0.877	1.4657	2.4385	3.4972 5.3717	4.4580	5.1302	-25.56	6.1879°	3.6	15.99dB	4
GA/L1	12	0.834	1.4467	1.9594	2.9607 5.118	3.9418	4.7224	-29.3	6.1879°	3.537	16.0dB	20

The proposed technique saves the number of antenna elements up to 45%. Consequently, the results of the proposed algorithm outperform the linear array optimization algorithm (GA/L1). Table 2 and Table 3 summarize a comparison between the synthesized beam against the Chebyshav array and GA/L1 in terms of excitation coefficients, array gain, DRR, SLL, HPBW, and execution time.

3) SHAPED BEAM PATTERN

Fig. 6 shows the results of the shaped beam pattern [7] with $N = 16$ against the proposed algorithm with $N = 13$ and GA/L1 [7] with $N = 13$. The excitation coefficients magnitude and phase are listed in Table 4. The proposed GWO with $N = 13$, the proposed scheme, and GA/L1 introduce an excellent matched pattern to the desired elements array pattern ($N = 16$) mentioned in [7]. In addition, only six seconds are required for the proposed technique, which is less than the thirty seconds for the GA/L1 technique. Furthermore, as seen in Fig. 7, the synthesis of the necessary shaped beam pattern using just $N = 12$ elements demonstrated the superiority of the proposed GWO approach over the GA/L1 technique. It offers a 25% decrease in the total number of elements in the array. Furthermore, when comparing the synthesized arrays to the original array, the DRRs of the arrays created using the GA/L1 approach and the suggested GWO technique are 9.73 and 4.278, respectively. So, it is evident that the suggested method offers minimized DRR. Table 5 lists the element locations and synthesized excitation coefficients. We also reduce the number of antennas to $N = 11$ with DRR = 6.28. This result is better than GA/L1 with $N = 12$. These results show that the proposed GWO has significant enhancement in performance over the linear array optimization algorithm (GA/L1). The results are listed in Table 6. Finally, the proposed scheme provides the best outcomes over GA/L1 [3].

B. REDUCING PEAK OF SLL (MATLAB SIMULATIONS)

1) 10-ELEMENT ULA PATTERN SYNTHESIS

Table 7 displays the optimization result for the $N = 10$ elements ULA that was produced by the proposed GWO and IWO [15]. The highest SLL of the original array is

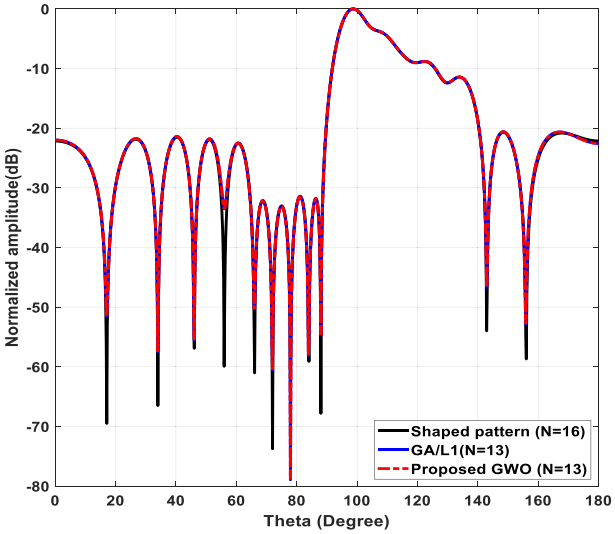

FIGURE 6. Synthesized radiation patterns of the proposed GWO with 13-element unequally spaced against shaped beam pattern.

TABLE 4. The created wide beam pattern parameters for N = 13 elements.

n	d/λ	$\lvert a_s \rvert$	$\angle a_s$
1	0.662	0.359	-69.7404
2	1.217	0.5115	11.9129
3	1.913	0.6911	44.9431
4	2.615	1.0201	86.6177
5	3.202	1.1631	150.9365
6	3.81	0.8482	-152.0306
7	4.33	0.2240	-92.9993
8	4.85	0.3296	-150.2879
9	5.556	0.4228	-122.1946
10	6.241	0.3284	-75.4453
11	6.876	0.2200	-42.6106
12	7.586	0.0897	-92.4306
13	8.139	0.2239	-3.3671

−12.9672 dB, whereas the peak SLL of the optimized array produced by the proposed GWO is −26.621 dB. As shown in Table 7, the proposed GWO algorithm obtained a peak of SLL less than IWO [15] by 0.071 dB, saving up to 50% in execution time. In addition, the HPBW of IWO is greater than the proposed GWO. So, the proposed algorithm outperforms IWO in [15] and ULA [9]. The radiation pattern achieved by the proposed GWO in comparison to other methods is shown in Fig. 8. The accuracy of the proposed algorithm is significantly higher than IWO. The proposed GWO is preferred over other methods because of its higher gain, with a LMSE of $8.25E-13$. The main lobe of the proposed algorithm is very close to the ULA, unlike IWO. Furthermore, the IWO saves the same interelement spacing of ULA $d = 0.5\lambda$ but in the proposed scheme, the interelement-spacing $d = 0.55\lambda$. Moreover, from the results of the proposed algorithm, it is clear that it outperforms the linear array optimization algorithm called IWO. The excitation coefficient, element spacing, SLL, HPBW, DRR, gain, and execution time are summarized in Table 7.

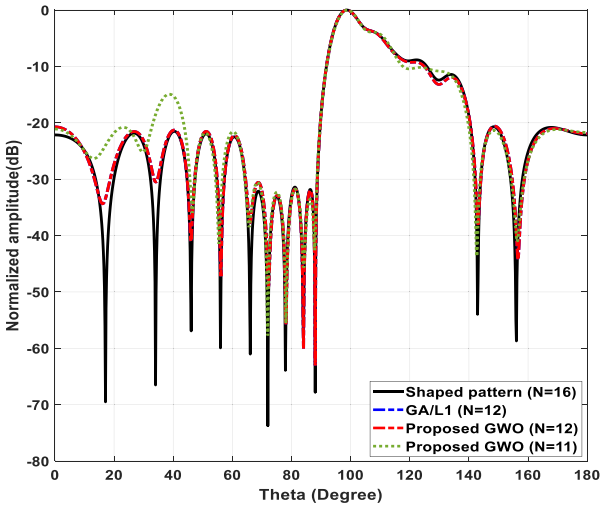

FIGURE 7. Synthesized radiation patterns of the proposed GWO with 12-elements and 11-elements unequally spaced against shaped beam radiation pattern.

TABLE 5. The created wide beam pattern parameters for N = 12 elements.

n	d/λ	$\lvert a_n \rvert$	$\angle a_s$
1	0.5580	0.3611	-64.3751
2	1.2550	0.4076	6.8524
3	1.9580	0.6617	35.1322
4	2.5450	0.9056	82.5040
5	3.1560	1.0269	137.6605
6	3.6770	0.8704	-169.1444
7	4.1840	0.4922	-143.9244
8	4.8940	0.4248	-115.6741
9	5.5800	0.2420	-104.7759
10	6.2150	0.3243	-84.9195
11	6.9250	0.2099	-42.3709
12	7.4790	0.2125	-6.4517

TABLE 6. The created wide beam pattern parameters for N = 11 elements.

n	d/λ	$\lvert a_n \rvert$	$\angle a_s$
1	0.8300	0.3996	-48.0338
2	1.5600	0.5684	27.7244
3	2.3620	0.7820	55.5868
4	3.0320	1.1641	108.4004
5	3.6420	1.1732	176.9404
6	4.3020	0.6889	-127.4435
7	5.1920	0.3752	-124.4878
8	6.0020	0.3587	-105.2641
9	6.7820	0.2991	-73.1755
10	7.2850	0.1864	-25.7811
11	8.1940	0.1957	5.9642

2) 20-ELEMENT ULA PATTERN SYNTHESIS

Using the Proposed GWO and another method, a 20-element symmetrical ULA optimization with equal spacing is optimized for the minimization of peak SLL. The result of the proposed GWO is very good compared to IWO, as shown in Fig. 9. The SLL of the ULA [3] is −13.19 dB, while the proposed scheme provides SLL equal to −35.69 dB with the same HPBW = 5.22°. The SLL obtained from IWO is −33.33 dB with HPBW = 5.58°. This means that the proposed GWO has better results than IWO [15]. Furthermore, the proposed optimization result gives the gain of the antenna array higher than IWO by 0.23 dB while

TABLE 7. Feeding amplitudes, d/λ, HPBW, SLL, and DRR the proposed GWO and IWO techniques compared to the ULA for N = 10 elements.

Algorithm	N	d/λ	Excitation coefficients					SLL (dB)	HPBW	DRR	Gain (dB)	Execution time (s)
ULA	10	0.5	1	1	1	1	1	-12.9672	10.26	1	10	0
IWO	10	0.49	0.9647	0.86648	0.6806	0.4625	0.3235	-26.55	11.34	2.9	8.19	5.8
Proposed GWO	10	0.55	0.999	0.891	0.7043	0.4789	0.345	-26.621	10.26	2.9	8.34	2.9

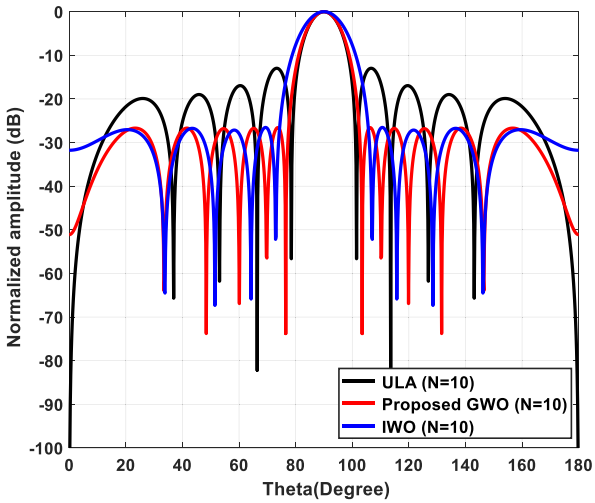

FIGURE 8. Synthesized patterns of the proposed GWO technique and IWO technique for SLL reduction with N = 10-elements.

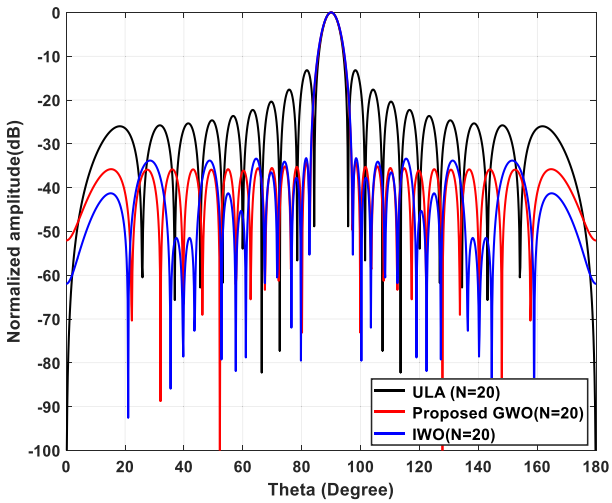

FIGURE 9. Synthesized patterns of the proposed GWO technique and IWO technique for SLL reduction with N = 20-elements.

the DRR is less than IWO. The gain of IWO is 10.61 dB, while the gain of the proposed scheme is 10.84 dB. Also, the DRR of the IWO and proposed scheme are 6.6 and 5.2, respectively. The excitation coefficient, element spacing, SLL, HPBW, DRR, gain, and execution time are summarized in Table 8. Furthermore, Fig. 9 shows the field pattern of the proposed scheme versus the original pattern of ULA and another method in [15] for $N = 20$. The results show that the HPBW of the proposed scheme is identical to the HPBW of the ULA, unlike the IWO. So, the proposed algorithm has better improvement than the linear array optimization algorithm (IWO)

3) 16-ELEMENT ULA PATTERN SYNTHESIS

Fig. 10 presents the results of the radiation pattern for ULA, IWO, and the proposed GWO for $N = 16$ element, respectively. It saves the execution time to obtain the result up to 50%. From the comparison, it is clear that the proposed scheme achieves the best performance. The SLL of the ULA is -13.1491 dB, while the SLL of the proposed GWO and IWO are -48.7 dB and -27.65 dB, respectively. So, the proposed scheme has a peak of SLL less than IWO [15] by 21.1 dB and less than ULA by 35.55 dB. In addition, the HPBW of the proposed scheme is identical to ULA, unlike IWO, which has a higher HPBW than ULA by 1.44°. Furthermore, the proposed scheme has a higher gain than IWO by 0.9329 dB, but DRR is higher. Table 9 lists the excitation coefficient, element spacing, SLL, HPBW, DRR, gain, and execution time. Finally, the proposed scheme is very close to ULA with the lowest SLL compared to IWO and ULA. In addition, the proposed algorithm gives improved results than the linear array optimization algorithm called IWO.

4) 32-ELEMENT ULA PATTERN SYNTHESIS

The results of the radiation pattern for ULA, IWO, and proposed GWO are presented in Fig. 11 for $N = 32$ element. It achieves savings in the execution time up to 30%. From the comparison, it is clear that the proposed scheme performs the best performance. The SLL of the proposed GWO is -38.019 dB while the SLL of the ULA and IWO are -13.2592dB and -30.1 dB, respectively. Consequently, the proposed scheme has a peak of SLL less than IWO [15] by 8dB and less than ULA by 24.75 dB. Also, the HPBW of the proposed scheme is identical to ULA, unlike IWO which has a higher HPBW than ULA by 1.08°. Furthermore, the proposed scheme has a higher gain than IWO by 0.37dB but DRR is higher. Finally, we can say the proposed GWO gives great results than ULA [9] and IWO [15]. Table 10 lists the

TABLE 8. Feeding amplitudes, d/λ, HPBW, SLL, and DRR the proposed GWO and IWO techniques compared to the ULA for N = 20 elements.

Algorithm	N	d/λ	Excitation coefficients					SLL (dB)	HPBW	DRR	Gain (dB)	Execution time (s)
ULA	20	0.5	1	1	1	1	1	-13.19	5.22	1	13.01	0
			1	1	1	1	1					
IWO	20	0.55	0.9453	0.9262	0.8805	0.7420	0.66805	-33.33	5.58	6.6	10.61	4.83
			0.5427	0.4061	0.2941	0.2176	0.143					
Proposed GWO	20	0.65	0.9989	0.9658	0.8971	0.8023	0.6892	-35.69	5.22	5.2	10.84	3.1
			0.5643	0.43821	0.322	0.219	0.1834					

TABLE 9. Feeding amplitudes, d/λ, HPBW, SLL, and DRR the proposed GWO and IWO techniques compared to the ULA for N = 16 elements.

Algorithm	N	d/λ	Excitation coefficients				SLL (dB)	HPBW	DRR	Gain (dB)	Execution time (s)
ULA	16	0.5	1	1	1	1	-13.1491	6.30	1	12.0412	
			1	1	1	1					0
IWO	16	0.6	0.9898	0.9607	0.8716	0.8449	-27.65	7.74	9.8	9.2184	5.8
			0.7230	0.5730	0.4807	0.1816					
Proposed GWO	16	0.77	0.981	0.9219	0.7795	0.6014	-48.7	6.3	14.5	10.1513	
			0.4182	0.2560	0.1322	0.0673					2.9

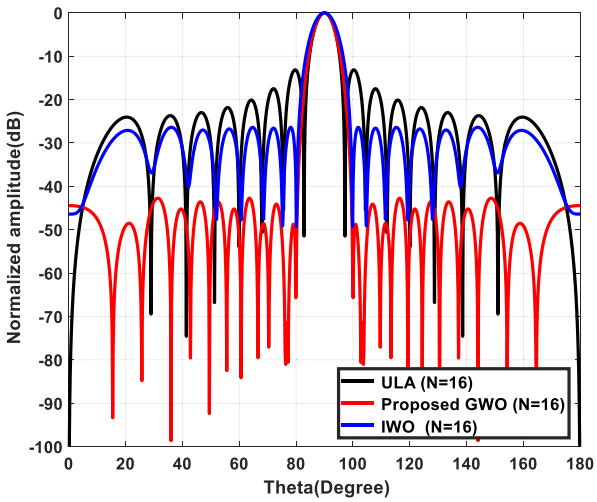

FIGURE 10. Synthesized patterns of the proposed GWO technique and IWO technique for SLL reduction with N = 16-elements.

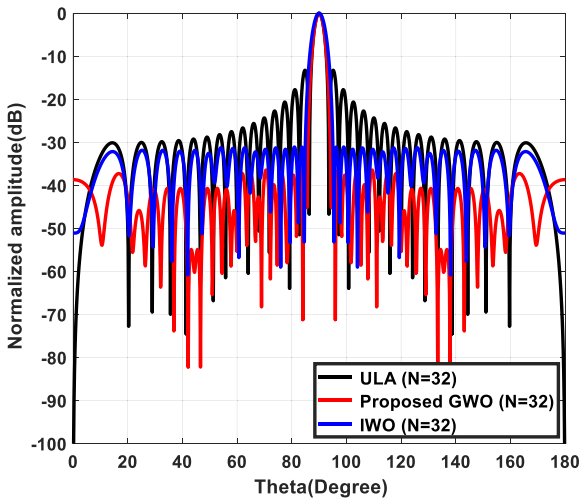

FIGURE 11. Synthesized patterns of the proposed GWO technique and IWO technique for SLL reduction with N = 32 elements.

excitation coefficient, element spacing, SLL, HPBW, DRR, gain, and the execution time.

C. REDUCING PEAK OF SLL (CST SIMULATIONS)

The obtained results from the proposed GWO (excitation coefficients and interelement spacing) can be initially checked to be acceptable for practical applications using computer simulation technology (CST). These results were used to design and feed LAA on CST. CST microwave studio software package is used to build a half wavelength dipole (λ/2) element in order to practically validate the suggested methodologies. Fig. 12 displays the dimensions of the dipole elements as well as the E-plane pattern. There is a 10 mm dipole diameter. While Fig. 13 displays the scattering parameter |S11| versus the dipole's frequency, it is evident that the dipole has a resonance frequency of $f_O = 1$ GHz.

1) 10-ELEMENT ULA PATTERN SYNTHESIS

This section verifies the effectiveness and viability of the proposed GWO technology employing CST and a dipole antenna element in place of an isotropic antenna. Fig. 14 (a) and (b) show the polar plots of the original and synthesized ULA patterns in the E-plane for 10-element, respectively. Through analysis of the data, it appears that the implemented patterns by the proposed GWO yield an SLL of −26.6 dB, which is higher than the ULA pattern

TABLE 10. Feeding amplitudes, d/λ, HPBW, SLL, and DRR the proposed GWO and IWO techniques compared to the ULA for N = 32 elements.

Algorithm	N	d/λ	Excitation coefficients				SLL (dB)	HPBW	DRR	Gain (dB)	Execution time (s)
ULA	32	0.5	1	1	1	1	-13.2592	3.06	1	15.0515	0
			1	1	1	1					
			1	1	1	1					
			1	1	1	1					
IWO	32	0.6	0.9969	1.0000	0.9757	0.9049	-30.1	4.14	9.8	12.8059	10
			0.8317	0.8317	0.7572	0.7039					
			0.6628	0.5290	0.4582	0.4497					
			0.3931	0.2831	0.1987	0.3559					
Proposed GWO	32	0.7	0.9999	0.9999	0.9999	0.9358	-38.019	3.06	14.5	13.1836	7
			0.8710	0.8107	0.7273	0.6250					
			0.5802	0.4901	0.427	0.34					
			0.2672	0.153	0.1399	0.1381					

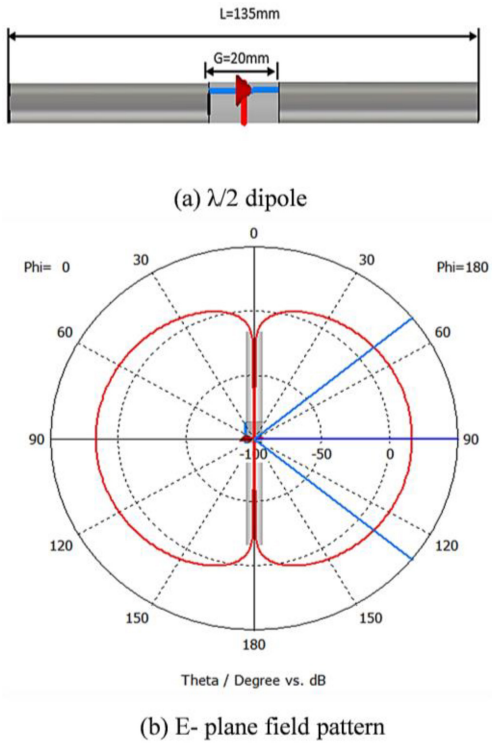

FIGURE 12. Dipole antenna.

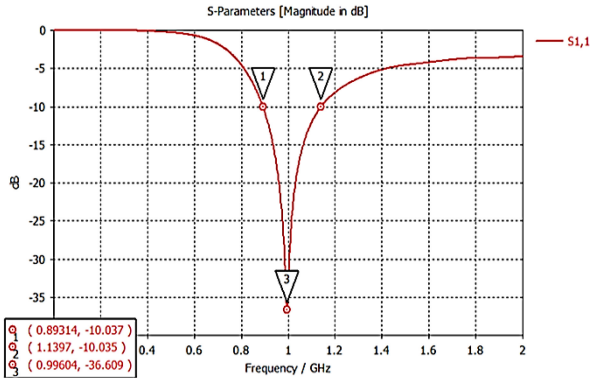

FIGURE 13. Scattering parameter |S11| versus dipole antenna frequency.

double drop in SLL, which equals −13.2 dB. Furthermore, the HPBW of the proposed scheme and the original pattern are very close to each other. Moreover, the main lobe magnitude of the proposed GWO is greater than that obtained by ULA.

2) 16-ELEMENT ULA PATTERN SYNTHESIS

This section verifies the effectiveness and viability of the proposed GWO technology employing CST for 16-element. The polar plots of the ULA and synthesized patterns in the E-plane are displayed in Fig. 15 (a) and (b), respective. Data analysis suggests that the proposed GWO gives an SLL of −40.8 dB, while the ULA gives −13.2 dB. The reduction in the SLL is up to 68.13%. Moreover, there is a strong similarity between the original pattern and the suggested scheme's HPBW. Furthermore, the predicted GWO's main lobe magnitude is larger than ULA, as shown in Fig. 15 (a) and (b).

3) 20-ELEMENT ULA PATTERN SYNTHESIS

The usefulness and feasibility of the suggested GWO technology, which uses CST for 20 elements, are confirmed in this section. Fig. 16 (a) and (b) show the polar plots of the ULA and synthesized patterns in the E-plane, respectively. Data analysis reveals that the suggested GWO generates an SLL of −34.3 dB, whereas the ULA gives −13.2dB. The reduction in SLL is up to 62%. Furthermore, there exists a good correspondence between the HPBW of the proposed scheme and the original pattern. Additionally, as seen in Fig. 16 (a) and (b), the main lobe magnitude of the proposed GWO is bigger than ULA.

4) 32-ELEMENT ULA PATTERN SYNTHESIS

As mentioned in the previous sections, using CST for 32 elements, this part confirms the effectiveness and viability of the proposed GWO technique. Fig. 17 (a) and (b) show the polar plots of the ULA and the synthesized patterns in the E-plane, respectively. Examining the outcomes, it is evident that the suggested GWO generates an SLL of −35.2 dB, whereas the ULA gives −13.2 dB. The reduction

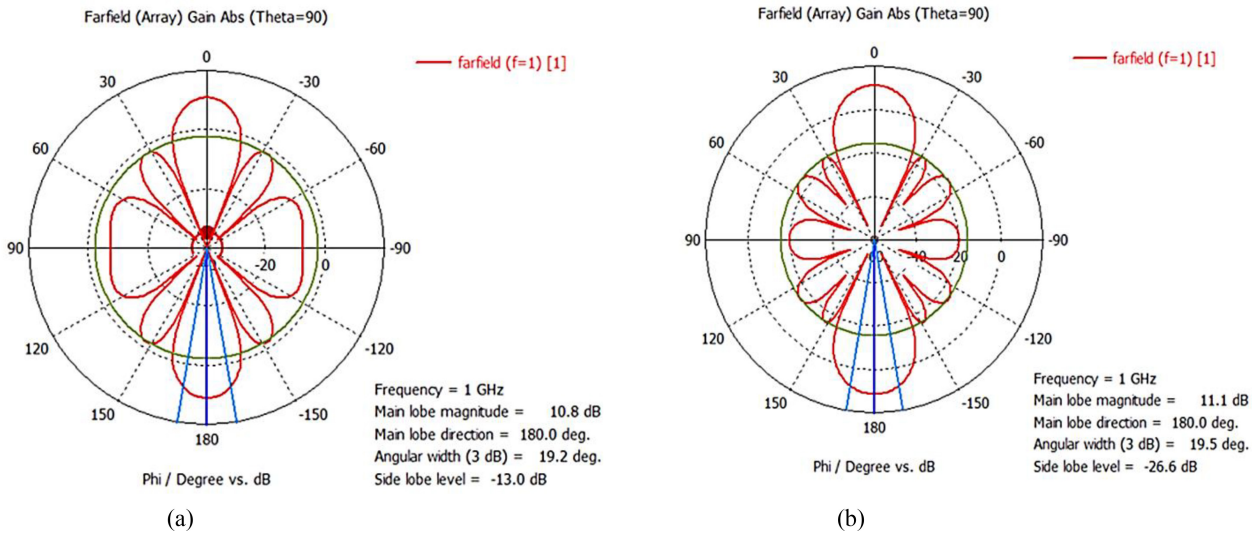

FIGURE 14. Polar plot of ULA versus proposed GWO by CST program for N = 10.

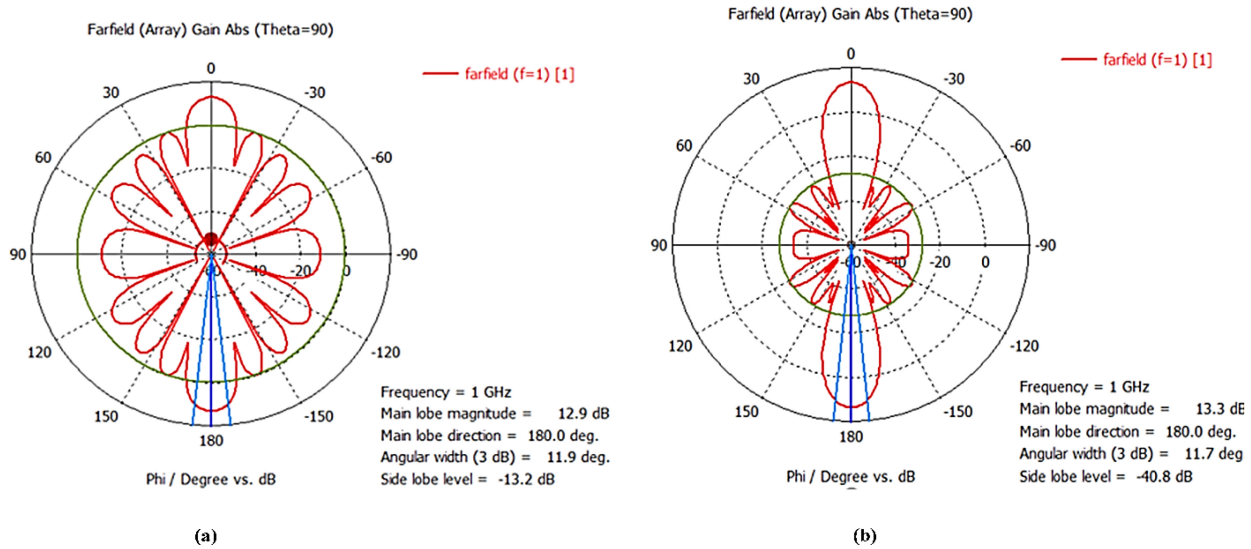

FIGURE 15. Polar plot of ULA versus proposed GWO by CST program for N = 16.

in SLL is up to 62.5%. Furthermore, the original pattern and the HPBW of the proposed system are quite comparable. As seen in Fig. 17 (a) and (b), the main lobe magnitude of the anticipated GWO is also greater than ULA. So, the proposed scheme is applicable practically, which gives excellent results.

Finally, the MA [13], IWO [15], FA [46], MFO [34], and PSO [36] state-of-the-art approaches are compared with the suggested SLL reduction strategies for ULA with 10, 16, 20, and 32 elements with $d = 0.5\lambda$. The synthesized pattern with proposed GWO Fig. 8, Fig. 9, Fig. 10, and Fig. 11. Consequently, Table 11. Shows the SLL of it is much lower than other algorithms in comparison. In addition, compared to other strategies, the presented techniques have the shortest runtime.

VI. MIMO SYSTEM MODEL AND THEORETICAL ANALYSIS

In this section, the digital precoding in mmWave system has high cost and power consumption [40] while analog precoding has bad performance. Consequently, Hybrid beamforming is the better choice for overcoming the constraints of pure digital or analog beamforming in communication systems. It reduces the needed RF chains, in addition, analog phase shifters can be used for the implementation of analog beamforming. As an application of the hybrid beamforming approach, the proposed GWO utilized for digital beamforming. The role of using the proposed GWO in this part is obtaining the excitation coefficients of transmitting antennas and interelement spacing between them. This will maximize the gain of the system. This can be done as the following:

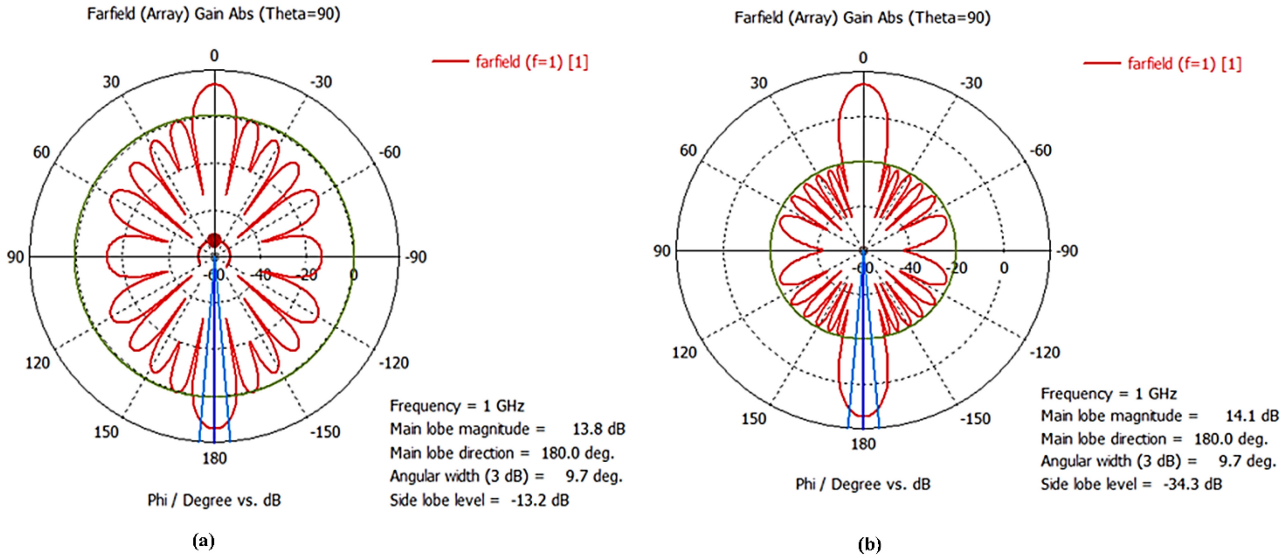

FIGURE 16. Polar plot of ULA versus proposed GWO by CST program for N = 20.

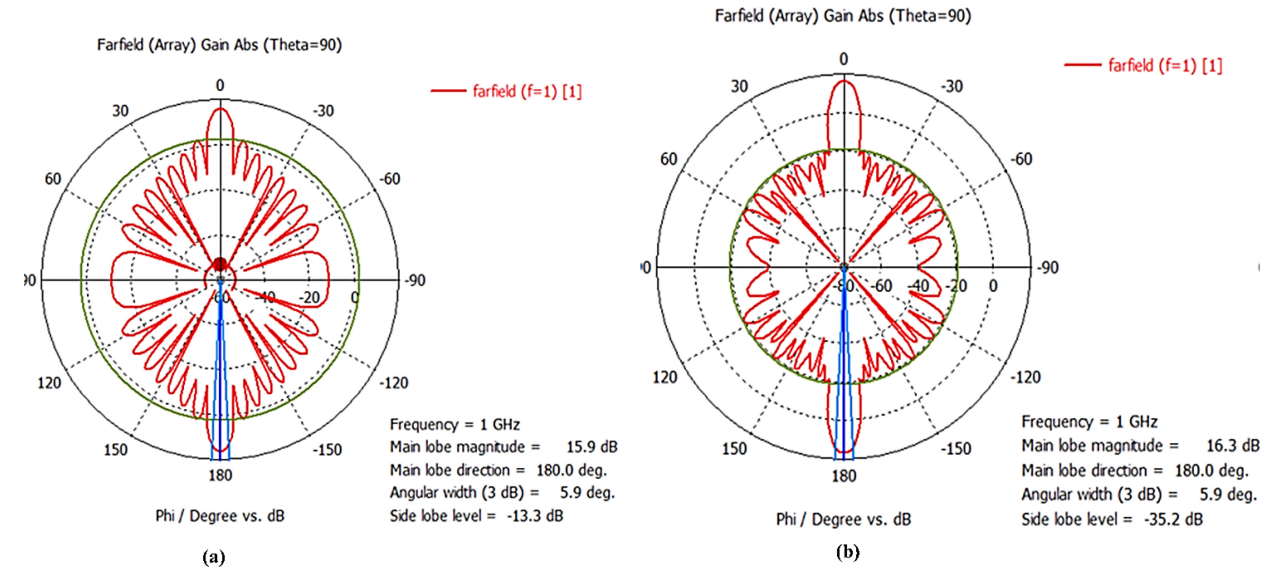

FIGURE 17. Polar plot of ULA versus proposed GWO by CST program for N = 32.

In the mmWave MIMO system shown in Fig. 1, the base station (BS) is connected to a transmission antenna (N_t) and an RF chain (N_D) transmits a data stream (N_S) to the reception antennas (N_r). When $N_S \leq N_D \leq N_t$, data streams are first broadcast to RF chains by a $N_D \times N_S$ digital precoding matrix. APSs, and variable attenuators are used to accomplish an $N_t \times N_D$ analog precoding matrix V_A. A beamforming matrix determines how each RF chain is distributed across the array's antenna elements. The following can be used to represent the received signal, r:

$$\mathbf{r} = \sqrt{\beta}\mathrm{HD}\mathbf{V_A}\mathbf{V_D}\mathbf{x} + \mathbf{z} \tag{14}$$

where $\mathbf{r} \in \mathbb{C}^{\mathbf{N_r}\times\mathbf{1}}$ is the received signal at the receiver side, and $\beta = P/N_o$ is the average SNR. $z \in \mathbb{C}^{N_r\times 1}$ is a Gaussian noise vector with $\mu = 0$ and $\sigma^2 = \mathbf{1}$. The digital beam forming matrix $\mathbf{D} \in \mathbb{C}^{N_t\times N_t}$ is written as:

$$\mathbf{D} = \begin{bmatrix} a_1 & \cdots & a_1 \\ \vdots & \ddots & \vdots \\ a_{N_t} & \cdots & a_{N_t} \end{bmatrix} \tag{15}$$

where $a_1,\ a_2,\ a_3, \ldots, a_{N_t}$ ae the excitation coefficient for N_t transmit antennas obtained by proposed GWO.

The transmitted signal vector can be written as:

$$\mathbf{x} = [\mathbf{x_1},\ \mathbf{x},\ \mathbf{x_3},\ \ldots, \mathbf{x_{N_S}}]^{\mathbf{T}} \tag{16}$$

The MIMO channel matrix $\mathbf{H} \in \mathbb{C}^{N_t\times N_r}$ is normalized such that $\mathbf{E}\left[\|\mathbf{H}\|^2\right] = \mathbf{N_t N_r}$ and it can be given by [42].

$$\mathbf{H}(t) = \sqrt{\frac{N_t N_r}{L\ L_c}} \sum_{i=1}^{L} \sum_{j=1}^{\mathrm{Lc}} \alpha_{i,j} \mathbf{a}_r\left(\theta_{ij}^a\right) \mathbf{a}_t^*\left(\theta_{ij}^d\right) \tag{17}$$

TABLE 11. Comparison between proposed algorithms against different optimization algorithms.

Algorithm	Array length	SLL(dB)	Execution time(s)
ULA [8]	10	-12.97	0
ULA [8]	16	-13.15	0
ULA [8]	20	-13.22	0
ULA [8]	32	-13.25	0
IWO [15]	10	-26.55	3.49
IWO [15]	16	-35.21	7.47
IWO [15]	20	-33.33	4.83
IWO [15]	32	-28.19	11.89
PSO [36]	10	-25.53	2.78
PSO [36]	16	-17.17	4.35
PSO [36]	20	-25.92	5.37
PSO [36]	32	-25.05	9
MFO [34]	10	-26.62	2.75
MFO [34]	16	-40.68	5.58
MFO [34]	20	-32.03	5.00
MFO [34]	32	-25.45	9.59
MA [13]	10	-26.7	9.99
MA [13]	16	-48.27	14.13
MA [13]	20	-34.9	16.26
MA [13]	32	-35.73	27.17
FA [46]	10	-26.64	24.95
FA [46]	16	-46.28	52.52
FA [46]	20	-34.76	56.77
FA [46]	32	-28.32	88.98
Proposed GWO	10	-26.8	2.9
Proposed GWO	16	-48.7	2.9
Proposed GWO	20	-35.69	3.1
Proposed GWO	32	-38.019	7

where L is the number of paths and L_c is the cluster numbers. $\alpha_{i,j}$ is the complex channel gain of i^{th} path and j^{th} cluster. $\left(\theta_{ij}^{a}\right)$ is a uniformly distributed angle of arrival (AOA) and $\left(\theta_{ij}^{d}\right)$ is a uniformly distributed angle of arrival (AOD). The beam steering vectors at UE and BS are denoted as $\mathbf{a}_r\left(\theta_{ij}^{r}\right) \in \mathbb{C}^{N_r \times 1}$ and $\mathbf{a}_t\left(\theta_{ij}^{t}\right) \in \mathbb{C}^{N_t \times 1}$ respectively. The normalized steering vectors are expressed as:

$$\mathbf{a}_t\left(\theta_{ij}^{t}\right) = \frac{1}{\sqrt{N_t}}\left[1 \; e^{jkd\sin(\theta_{ij}^{t})} \; \cdots \; e^{j(N_t-1)kd\sin(\theta_{ij}^{t})}\right]^T \quad (18)$$

$$\mathbf{a}_r\left(\theta_{ij}^{r}\right) = \frac{1}{\sqrt{N_r}}\left[1 \; e^{jkd\sin(\theta_{ij}^{r})} \; \cdots \; e^{j(N_r-1)kd\sin(\theta_{ij}^{r})}\right]^T \quad (19)$$

where d is the interelement spacing between antennas and $k = 2\pi/\lambda$ is the wave number with wavelength $\lambda = c/f (c = 3 \times 10^8 m/s$ and f is the frequency of operation). This study assumes that both the transmitter and receiver have perfect channel state information (CSI) and are perfectly synchronized. The estimated signal vector at user equipment after the analog and digital combining can be expressed as:

$$\mathbf{y} = \mathbf{U_D^H U_A^H} r \quad (20)$$

where, $\mathbf{U}_A \in N_\text{d} \times N_r$ and $\mathbf{U}_\text{d} \in N_\text{s} \times N_\text{d}$ are the analog and digital decoding matrices, respectively. The constraints of the analog decoder are $\left|\mathbf{U}_A^{\{i,j\}}\right| = 1/\sqrt{N_r}$. $(.)^H$ denotes the conjugate transpose. Thus, hybrid precoding's goal for MIMO systems is to maximize C through $\mathbf{D}$, $\mathbf{V}_\text{A}$, $\mathbf{V}_\text{d}$ $\mathbf{U}_\text{A}$ and $\mathbf{U}_\text{d}$ jointly. The rate of the PHB can be written as:

$$C = \log_2\left(\left|\mathbf{I}_{N_\text{s}} + \frac{\beta}{N_\text{s}}\mathbf{V}_n^{-1}\mathbf{U}_\text{d}^H\mathbf{U}_A^H\mathbf{H}\mathbf{D}\mathbf{V_A}\mathbf{V_D} \times \mathbf{V_D^H}\mathbf{V_A^H}\mathbf{H}^H\mathbf{U_A}\mathbf{U_D}\right|\right) \quad (21)$$

where the noise covariance matrix $\mathbf{V}_n$.

$$\mathbf{V}_n = \mathbf{V}_D^H\mathbf{V}_A^H\mathbf{H}^H\mathbf{U}_A\mathbf{U}_D \quad (22)$$

In this work, we use the mean square error MSE [44] as the performance metric for the combined transmit and receive PHB design. MSE can be calculated as:

$$MSE \triangleq E\left\{\left\|\delta^{-1}\mathbf{y}-\mathbf{x}\right\|^2\right\} \quad (23)$$

where δ is the scaling factor for optimizing PHB beamformers. From Eq. (14) and Eq. (20). Eq. (23) can be rewritten as:

$$\begin{aligned} MSE &\triangleq E\left\{\left\|\delta^{-1}\sqrt{\beta}\mathbf{U_D^H U_A^H}\mathbf{H}\mathbf{D}\mathbf{V_A}\mathbf{V_D}\mathbf{x}+\mathbf{U_D^H U_A^H}\mathbf{z}-\mathbf{x}\right\|^2 \\ &= tr\Big(\delta^{-2}\beta\mathbf{U_D^H U_A^H}\mathbf{H}\mathbf{D}\mathbf{V_A}\mathbf{V_D}\mathbf{V_D^H}\mathbf{V_A^H}\mathbf{D}^\text{H}\mathbf{H}^\text{H}\mathbf{U_A}\mathbf{U_D} \\ &\quad -\delta^{-1}\sqrt{\beta}\mathbf{U_D^H U_A^H}\mathbf{H}\mathbf{D}\mathbf{V_A}\mathbf{V_D}\Big) \\ &\quad -\delta^{-1}\sqrt{\beta}\mathbf{V_D^H}\mathbf{V_A^H}\mathbf{D}^H\mathbf{H}^\text{H}\mathbf{U_A}\mathbf{U_D} \\ &\quad +\sigma^2\delta^{-2}\mathbf{U_D^H U_A^H}\mathbf{U_A}\mathbf{U_D} + \mathbf{I_{N_s}} \end{aligned} \quad (24)$$

Analog beamformers rely on phase shifters to alter input signal phases, hence their components must adhere to the constant modulus requirement as $\left|[\mathbf{V_A}]_{i,j}\right| = 1$ for $i = 1, 2, \ldots, N_t$ and $j = 1, 2, \ldots, N_\text{d}$, and $|[\mathbf{U_A}]_\text{mn}| = 1$ for $m = 1, 2, \ldots, N_r$ and $n = 1, 2, \ldots, N_\text{d}$. From Eq. (24), with the transmit power and phase shifter constant modulus constraints, the HBF optimizer issue may be expressed as follows:

$$\begin{aligned} &\underset{\{\mathbf{V_d},\mathbf{V}_A,\mathbf{D},\mathbf{U}_A,\mathbf{U_d},\delta\}}{\text{argmin}} \quad \text{MSE} \\ &\text{subject to } \|\mathbf{V}_A\mathbf{V_D}\|_F^2 = 1, \; \left|[V_A]_{i,j}\right|^2 \\ &= 1 \; \forall \; i,j; \; |[U_A]_{mn}|^2 = 1 \; \forall \; m,n \end{aligned} \quad (25)$$

where $\|.\|_F$ is the standard Forbenius norm. However, in order to raise the potential channel SE in Eq. (21) for hybrid beamforming in the multiuser situation, the joint optimization problem will be stated as follows:

$$\begin{aligned} &\underset{\{\mathbf{V_d},\mathbf{V}_A,\mathbf{D},\mathbf{U}_A,\mathbf{U_d}\}}{\text{argmax}} \quad C(\mathbf{x},\widehat{\mathbf{x}}) \\ &\text{subject to } \|\mathbf{A}\mathbf{V}_{RF}\mathbf{V}_{BB}\|_F^2 = 1 \end{aligned} \quad (26)$$

Furthermore, for comparison, the optimal optimization problem of the fully digital scenario is as follows:

$$\text{C}_\text{D} = \max_{\mathbf{V},\mathbf{U}} \; C(\mathbf{x},\widehat{\mathbf{x}})$$

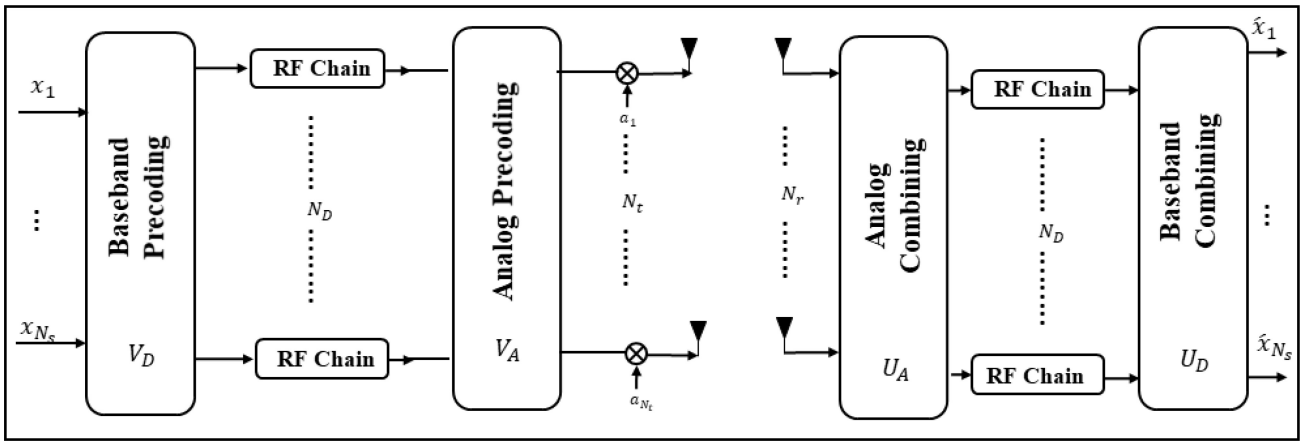

FIGURE 18. Block diagram of PHB for MIMO system.

$$\text{subject to} \quad \|\mathbf{V}\|_F^2 = 1 \tag{27}$$

where C_D is the Fully digital spectral efficiency [3], such that:

$$C_D = \log_2\left(\left|\mathbf{I}_{N_s} + \frac{\beta}{N_s}\mathbf{V}_n^{-1}\mathbf{U}^H\mathbf{H}\mathbf{V}\mathbf{V}^H\mathbf{H}^{\mathbf{H}}\mathbf{U}\right|\right) \tag{28}$$

$$\mathbf{V}_n = \mathbf{U}^H\mathbf{U} \tag{29}$$

$$\mathbf{SVD}(\mathbf{H}) = \mathrm{U}\Sigma\mathbf{V}^{\mathbf{H}} \tag{30}$$

where $\mathrm{rank}(\mathbf{H}) \geq N_s$, $\mathbf{U} \in N_r \times N_r$ is the unitary matrix for digital decoder, $\mathbf{V} \in N_t \times N_t$ is the unitary matrix for digital precoder, and $\Sigma \in N_r \times N_t$ is the diagonal matrix for the problem in Eq. (27). The digital precoder $\mathbf{V_D} \in N_t \times N_s$ and combiner $\mathbf{U_D} \in N_r \times N_s$ can be expressed as:

$$\mathbf{V_D} = \begin{bmatrix}\mathbf{V}_{N_s} \\ \mathbf{0}\end{bmatrix} \tag{31}$$

$$\mathbf{U_D} = \begin{bmatrix}\mathbf{U}_{N_s} \\ \mathbf{0}\end{bmatrix} \tag{32}$$

where $\mathbf{V}_{N_s}$ and $\mathbf{U}_{N_s}$ are the first N_s column $\mathbf{V}$ and $\mathbf{U}$ respectively. The Fully digital SE is expressed by:

$$C_D = \log_2\left(\left|\mathbf{I}_{N_s} + \frac{\beta}{N_s}\mathbf{\Sigma}^{\{1:N_s,1:N_s\}^2}\right|\right) \tag{33}$$

so,

$$C_D = \sum_{i_s}^{N_s}\log_2\left(1 + \frac{\beta}{N_s}\mathbf{\Sigma}^{\{i_s,i_s\}^2}\right) \tag{34}$$

VII. PROPOSED HYBRID BEAMFORMING DESIGN

Utilizing the N_t-elements of the current LAA, the proposed GWO performs digital beam forming at the BS to produce the same pattern of a much larger array of N elements such that:

$$\boldsymbol{AF}_s(\theta)|_{N_t} = \boldsymbol{AF}_d(\theta)|_N \tag{35}$$

where $N \gg N_t$ where. The solution to this problem is to optimize the excitation coefficients and element spacing of the antenna array. The result of that, the synthesized array gain η_s is very close to the desired array gain η_d, the synthesized gain $\eta_s \gg \eta$ (LAA with the same length of the synthesized antenna array) by a value of $\triangle\eta$ that is given by:

$$\triangle\eta = \eta_s - \eta_T \tag{36}$$

As a result, the SNR of PHB, called $\mathrm{SNR_{PHB}}$, will be increased by $\triangle\eta$ and interference will be decreased. Consequently, we tend now to design the proposed precoders and combiners according to new coefficients of analog precoders obtained from the proposed GWO.

It is doubtful that the PHB issue in Eq. (25) will discover the ideal solution because it entails a combined optimization across six variables and non-convex constraints. Dividing the original issue into two sub-problems that correspond to the optimization for the hybrid transmit precoder and receive combiner, respectively, and solving each one separately is a suboptimal but effective technique to get around the challenges.

A. HYBRID TRANSMIT PRECODER DESIGN

In this section, we focus on designing the transmit precoders $\mathbf{D}$, $\mathbf{V_A}$, and $\mathrm{V_D}$ in addition to δ. The combining matrix at the receiver is fixed. Let $\mathbf{V_n}$=$\mathbf{DV_A}$ and $\mathbf{V_m}$=δ $\mathbf{V_D}$. The precoder optimization is expressed as:

$$\begin{aligned}\min_{\mathbf{V_nV_m},}\ & \mathrm{tr}\Big(\mathbf{H}_t^{\mathrm{H}}\mathbf{V_n}\mathbf{V_m}\mathbf{V}_{\mathbf{m}}^{\mathbf{H}}\mathbf{V}_{\mathbf{n}}^{\mathbf{H}}\mathbf{H_t} - \mathbf{H}_t^{\mathrm{H}}\mathbf{V_n}\mathbf{V_m} - \mathbf{V}_{\mathbf{m}}^{\mathbf{H}}\mathbf{V}_{\mathbf{n}}^{\mathbf{H}}\mathbf{H_t} \\ & -\sigma^2\delta^{-2}\mathbf{U}^H\mathbf{U} + \mathbf{I_{N_S}}\Big) \\ \text{subject to}\ & \mathrm{tr}\ (\mathbf{V_nV_m}\mathbf{V}_{\mathbf{m}}^{\mathbf{H}}\mathbf{V}_{\mathbf{n}}^{\mathbf{H}}) \leq \delta^{-2} \\ & |[\mathbf{V_A}]_{i,j}| = 1 \quad \forall\ \mathrm{i,j}\end{aligned} \tag{37}$$

where $\mathbf{H_t} \triangleq \mathbf{HU_AU_D}$ is the equivalent channel matrix. First, we fix $\mathbf{V_n}$ to get the ideal digital precoding matrix $\mathrm{V_m}$. Next, we derive the resultant objective as a function of $\mathbf{V_n}$. Finally, we optimize $\mathbf{V_n}$ by further minimizing the objective with the constant modulus constraint. This is our optimization technique. Owing to the transmit power limitation, it can be demonstrated through contradiction

that the best outcome necessitates the highest possible total transmit power, meaning that the ideal δ is determined by:

$$\delta = (\text{tr } (\mathbf{V_n V_m V_m^H V_n^H}))^{-\frac{1}{2}} \tag{38}$$

Then, we can obtain the optimized value of $\mathbf{V_n}$ according to this equation [41]:

$$\mathbf{V_m} = \left(\mathbf{V_n H_t H_t^H V_n^H} + \sigma^2 \,\text{tr}\left(\mathbf{U_A^H U_D^H U_D U_A}\right)\mathbf{V_n^H V_n}\right)^{-1}\mathbf{V_n^H H_t} \tag{39}$$

By substituting $\mathbf{V_n}$ and δ in (37) and some derivations we get

$$\mathbf{V_n} \triangleq \text{tr}\left(\left(\mathbf{I_{N_S}} + \frac{1}{\sigma^2 \text{tr}\left(\mathbf{U_A^H U_D^H U_D U_A}\right)}\mathbf{H_t V_n}\left(\mathbf{V_n^H V_n}\right)^{-1}\mathbf{V_n^H}\right)^{-1}\right) \tag{40}$$

Now, we can reduce the optimization problem in (37) to

$$\begin{aligned} &\min_{\mathbf{V_n}} \quad \mathbf{V_n} \\ &\text{subject to} \quad \left|[\mathbf{V_A}]_{i,j}\right| = 1 \;\forall\; i,j \end{aligned} \tag{41}$$

and use Manifold optimization to solve this problem and obtain the analog precoder matrix.

B. HYBRID RECEIVE COMBINER DESIGN

In this section, we focus on designing the transmit combiners $\mathbf{U_A}$ and $\mathbf{U_D}$. The precoding matrix at the transmitter is fixed. The optimization problem is expressed as:

$$\begin{aligned} &\min_{\mathbf{U_A},\mathbf{U_A}} \quad \text{tr}\left(\mathbf{U_r^H H_r H_r^H U_r} - \mathbf{U_r^H H_r} - \mathbf{H_r^H V_r} - \sigma^2\delta^{-2}\mathbf{U_r^H U_r} + \mathbf{I_{N_S}}\right) \\ &\text{subject to} \quad \left|[\mathbf{U_A}]_{m,n}\right| = 1 \;\forall\; m,n \end{aligned} \tag{42}$$

where $\mathbf{H_r} \triangleq \mathbf{H V_n V_m}$ and $\mathbf{U}_r \triangleq \mathbf{U_A U_D}$. Then, the objective function of 42 is differentiating concerning $\mathbf{U_D}$ and setting the result to zero to obtain the optimal $\mathbf{U_D}$ as follows:

$$\mathbf{U_D} = \left(\mathbf{U_A^H H_r H_r^H U_A} + \sigma^2\ \delta^{-2}\ \mathbf{U_A^H U_A}\right)^{-1}\mathbf{U_A^H H_r} \tag{43}$$

By substituting $\mathbf{U_D}$ in (41) we get

$$\begin{aligned} &\min_{\mathbf{U_A}} \quad \mathbf{U_A} \triangleq \text{tr}\left(\left(\mathbf{I_{N_S}} + \sigma^{-2}\,\delta^2 \mathbf{H_r^H U_A} \times \left(\mathbf{U_A^H U_A}\right)^{-1}\mathbf{U_A^H H_r}\right)^{-1}\right) \\ &\text{subject to} \quad \left|[\mathbf{U_A}]_{m,n}\right| = 1 \;\forall\; m,n \end{aligned} \tag{44}$$

VIII. NUMERICAL RESULTS OF THE PROPOSED PHB

To illustrate the effectiveness of the PHB structures for the multi-stream mmWave massive MIMO system, the simulation results of 1000 Monte Carlo iterations used to plot the SE against SNR are shown in this section. We also compare these results with the fully digital and the algorithms used in [3] and [43]. Numerical results for 32 × 16, 32 × 8, and 20 × 8 MIMO systems are obtained. Within the interval [0, π], the angles of arrivals and departures (AOAs/AODs) are evenly distributed. The path loss exponent of the system is n =4 [43]. Assuming an average noise power of $N_o = 1$. The PHB structure is put into practice by employing a conventional ULA at the reception side and non-uniform feeding of an LAA with equal spacing at the transmitter side.

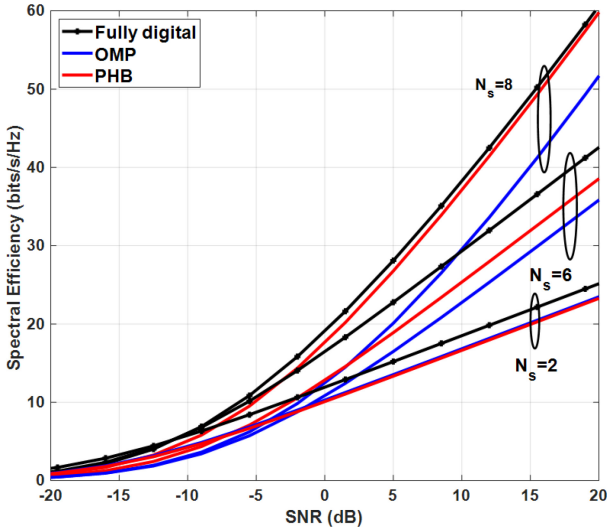

FIGURE 19. SE performance at different data steam of 32 × 16 MIMO for proposed PHB structure at L = 8 paths, N_D= 8.

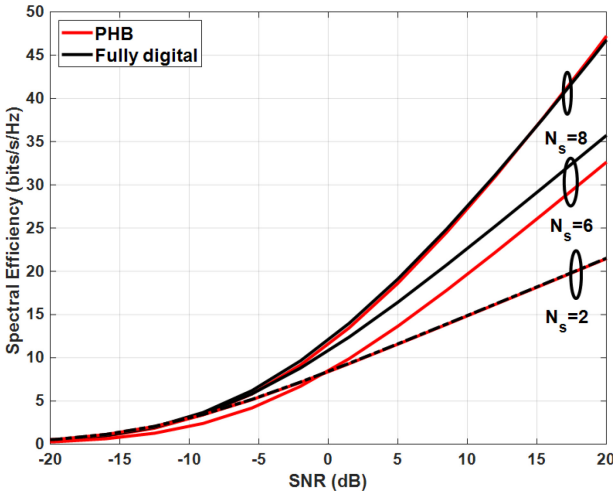

FIGURE 20. SE performance at different data streams of 32 × 8 MIMO for proposed PHB structure at L = 8 paths, N_D= 8.

A. STUDY THE EFFECT OF CHANGING N_S

Figs. 19, 20, and 21 present an analysis and clarification of the performance PHB structure versus fully digital elements [3] based on 32×16, 32×8, and 20×8 MIMO systems operating at various bitstreams counts $N_s = 2$, 4, and 8 while $N_d = 8$. These schemes are simulated at multipath channel $L = 8$ paths. The outcome of the simulation demonstrates that an increase in data streams improves SE performance. In addition, the performance of the PHB structure is fully digital, which is considered optimal precoding with the highest SE. This is the outcome of increasing the number of bit streams (Ns) to get multiplexing gain. In addition, the acquired SE gain comes from the effectiveness of the proposed GWO. In 32 × 16 and 32 × 8 scenarios, these simulations are performed with $N_t = 60$ fully digital antennas, while PHB used only 32 antennas. Then, the proposed scheme saves up to 46% in the number of antennas,

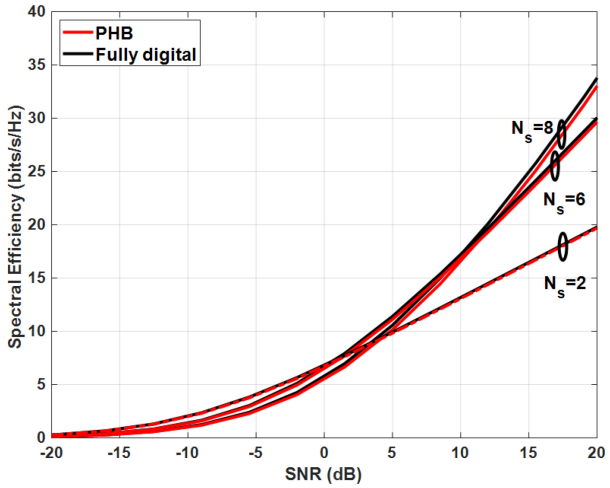

FIGURE 21. SE performance at different data streams of 20x8 MIMO for proposed PHB structure at L = 8 paths, N_D= 8.

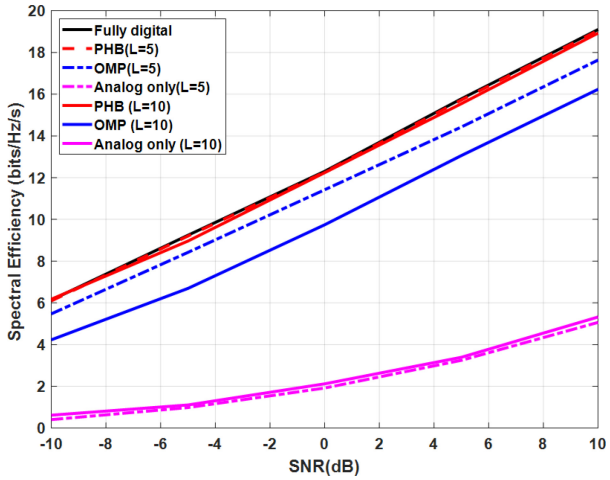

FIGURE 22. SE performance at different data streams of 32 × 16 MIMO for proposed PHB structure at L = 5, 10 paths, N_d = 2.

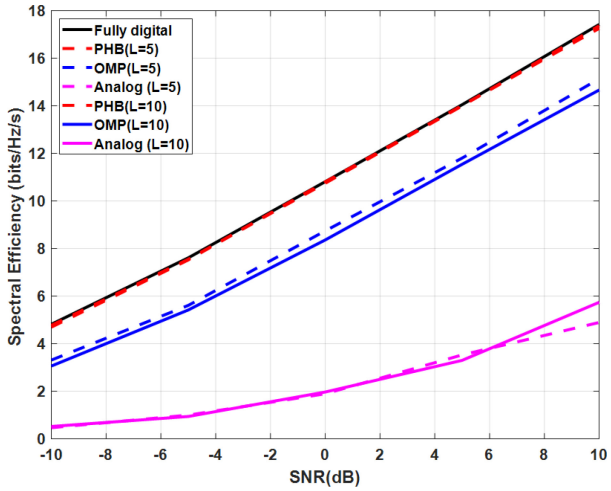

FIGURE 23. SE performance at different data streams of 32 × 8 MIMO for proposed PHB structure at L = 5, 10 paths, N_d = 2

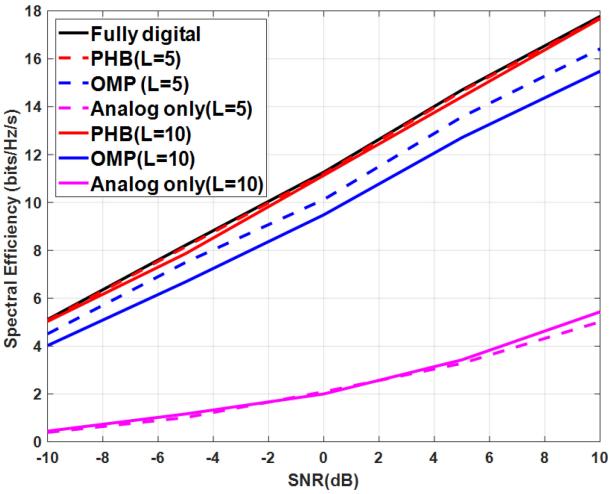

FIGURE 24. SE performance at different data streams of 20 × 16 MIMO for proposed PHB structure at L = 5, 10 paths, N_d = 2.

and consequently, it significantly reduces the hardware complexity of the proposed PHB. In addition, for the 20 × 8 scenario, the simulation is performed with $N_t = 42$ antennas of fully digital while PHB used only 20 antennas. Then, the proposed scheme saves up to 45% in the number of antennas. Also, it significantly reduces the hardware complexity of the proposed PHB.

B. STUDY THE EFFECT OF CHANGING L

Figs. 22, 23, 24, and 25 present an analysis and clarification of the performance proposed PHB structure versus Fully digital elements [3] and analog precoding only based 32 × 16, 32×8, 20×16 and 20×8 MIMO system at different numbers paths $L = 5$ and 10 while $N_d = 2$. These schemes are simulated at data steam $N_s = 2$ bits. The fully digital uses 60 antennas opposite to 32 antennas in the proposed scheme for 32 × 16, and 32 × 8 scenarios. In addition, the fully digital uses 42 antennas against 20 antennas in the proposed scheme for 20 × 16, and 32 × 8 scenarios. The simulation is performed on the fully digital [41] analog precoding [44], and orthogonal matching pursuit (OMP) [3]. Reducing the number of pathways results in a large rise in SE. Based on the same number of pathways, data stream, and RF chains, the suggested PHB structures achieve more SE than any other techniques in [3], [43]. As a result, PHB attains superior performance and nearly reaches optimum efficiency.

IX. CONCLUSION

This work proposes a new beamforming technique for ULA, Chebyshev arrays, and shaped pattern arrays that reduces size and SLL up to 50%. This approach is done via a combination between the GWO and L_2-norm called proposed GWO. By maximizing element spacing, the GWO method modifies the HPBW. Consequently, when the number of antenna elements is reduced, the suggested GWO technique provides a very close beam pattern to the required radiation pattern with low complexity. Furthermore, it provides SLL reduction and

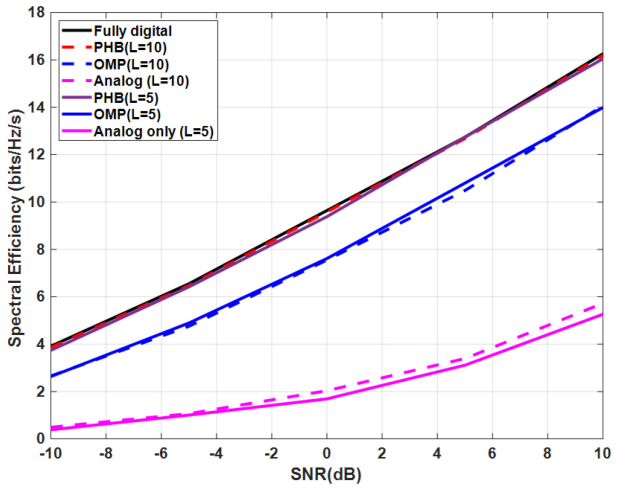

FIGURE 25. SE performance at different data streams of 20 × 16 MIMO for proposed PHB structure at $L = 5, 10$ paths, $N_d = 2$.

still has the same HPBW as the original radiation pattern unlike other algorithms mentioned in literature. In addition, the suggested methodologies are practically validated with the aid of the CST. Moreover, a PHB structure for MIMO systems is developed using the proposed GWO algorithm. It utilized the present number of antenna elements to maximize gain via apply beamforming to transmit antenna array. As well, it synthesizes the radiation pattern of significantly larger size and higher gain arrays without the need for additional elements. As a result, there are significant savings on antenna elements and related RF chains, which lowers system complexity. Moreover, maximizing array gain will raise the received SNR. Moreover, the SLL reduction scenario would improve system performance by reducing interference.

REFERENCES

[1] B. Ning et al., "Beamforming technologies for ultra-massive MIMO in terahertz communications," *IEEE Open J. Commun. Soc.*, vol. 4, pp. 614–658, 2023, doi: 10.1109/OJCOMS.2023.3245669.

[2] C. K. Sheemar, C. K. Thomas, and D. Slock, "Practical hybrid beamforming for millimeter wave massive MIMO full duplex with limited dynamic range," *IEEE Open J. Commun. Soc.*, vol. 3, pp. 127–143, 2022, doi: 10.1109/OJCOMS.2022.3140422.

[3] S. I. Farghaly, H. E. Seleem, M. M. Abd-Elnaby, and A. H. Hussein, "Pencil and shaped beam patterns synthesis using a hybrid GA/l optimization and its application to improve spectral efficiency of massive MIMO systems," *IEEE Access*, vol. 9, pp. 38202–38220, 2021, doi: 10.1109/ACCESS.2021.3063219.

[4] B S. Mirjalili, "Moth-flame optimization algorithm: A novel nature-inspired heuristic paradigm," *Knowl.-Based Syst.*, vol. 89, Nov. 2015, Art. no. 228249, doi: 10.1016/j.knosys.2015.07.006.

[5] F. Yang et al., "Synthesis of low-sidelobe 4-D heterogeneous antenna arrays including mutual coupling using iterative convex optimization," *IEEE Trans. Antennas Propag.*, vol. 68, no. 1, pp. 329–340, Jan. 2020, doi: 10.1109/TAP.2019. 2947153.

[6] H. Li, Y. Jiang, Y. Ding, J. Tan, and J. Zhou, "Low-sidelobe pattern synthesis for sparse conformal arrays based on PSO-SOCP optimization," *IEEE Access*, vol. 6, pp. 77429–77439, 2018, doi: 10.1109/ACCESS.2018.2883042.

[7] Y. Luo, N. Zhang, Z. N. Chen, W. An, K. Ma, and Q.-X. Chu, "A nonuniform compressed high-order mode dipole with sidelobe suppression," *IEEE Antennas Wireless Propag. Lett.*, vol. 21, pp. 2372–2376, 2022, doi: 10.1109/LAWP.2022.3193927.

[8] Q. Lou and Z. N. Chen, "Sidelobe suppression of metalens antenna by amplitude and phase controllable metasurfaces," *IEEE Trans. Antennas Propag.*, vol. 69, no. 10, pp. 6977–6981, Oct. 2021, doi: 10.1109/TAP.2021.3076312.

[9] A. Hussein, H. Abdullah, A. Salem, S. Khamis, and M. Nasr, "Optimum design of linear antenna arrays using a hybrid MoM/GA algorithm," *IEEE Antenna Wireless Propag. Lett.*, vol. 10, pp. 1232–1235, 2011, doi: 10.1109/LAWP.2011.2174189.

[10] P. Saxena and A. Kothari, "Optimal pattern synthesis of linear antenna array using grey wolf optimization algorithm," *Int. J. Antennas Propag.*, vol. 2016, Mar. 2016, Art. no. 1205970, doi: 10.1155/2016/1205970.

[11] A. A. M. El-Gaafary, Y. S. Mohamed, A. M. Hemeida, and A.-A. A. Mohamed, "Grey wolf optimization for multi-input multi-output system," *Univ. J. Commun. Netw.*, vol. 3, no. 1, pp. 1–6, 2015, doi: 10.13189/ujcn.2015.030101.

[12] R. Bera, R. Lanjewar, D. Mandal, R. Kar, and S. P. Ghoshal, "Comparative study of circular and hexagonal antenna array synthesis using improved particle swarm optimization," *Procedia Comput. Sci.*, vol. 45, 2015, pp. 651–660, doi: 10.1016/j.procs.2015.03.126.

[13] E.O. Owoola, K. Xia, T. Wang, A. Umar, and R. G. Akindele, "Pattern synthesis of uniform and sparse linear antenna array using mayfly algorithm," *IEEE Access*, vol. 9, pp. 77954–77975, 2021, doi: 10.1109/ACCESS.2021.3083487.

[14] Y. Liu, Y. Chai, B. Liu, and Y. Wang, "Bearing fault diagnosis based on energy spectrum statistics and modified mayfly optimization algorithm," *Sensors*, vol. 21, no. 6, p. 2245, Mar. 2021, doi: 10.3390/s21062245.

[15] G. Su et al, "An antenna array sidelobe level reduction approach through invasive weed optimization," *Int. J. Antennas Propag.*, vol. 2018, p. 116, Feb. 2018, doi: 10.1155/2018/4867851.

[16] S. Karimkashi and A.A.Kishk, "Invasive weed optimization and its features in electromagnetics," *IEEE Trans. Antennas Propag.*, vol. 58, no. 4, pp. 1269–1278, Apr. 2010, doi: 10.1109/TAP.2010.2041163.

[17] L. I. Wong, M. Sulaiman, M. Mohamed, and M. Hong, "Grey Wolf Optimizer for solving economic dispatch problems," in *Proc. IEEE Int. Conf. Power Energy*, Kuching, Malaysia, 2010, pp. 150–154, doi: 10.1109/PECON.2014.7062431.

[18] H. M. Song, M. H. Sulaiman, and M. R. Mohamed, "An application of Grey Wolf optimizer for solving combined economic emission dispatch problems," *Int. Rev. Model. Simul.*, vol. 7, no. 5, pp. 838–844, 2014, doi: 10.15866/iremos.v7i5.2799.

[19] S. Mirjalili, S. M. Mirjalili, and A. Lewis, "Grey wolf optimizer," *Adv. Eng. Softw.*, vol. 69, p. 4661, Mar. 2014, doi: 10.1016/j.advengsoft.2013.12.007.

[20] P. Rocca, L. Poli, N. Anselmi, and A. Massa, "Nested optimization for the synthesis of asymmetric shaped beam patterns in subarrayed linear antenna arrays," *IEEE Trans. Antennas Propag.*, vol. 70, no. 5, pp. 3385–3397, May 2022, doi: 10.1109/TAP.2021.3137176.

[21] Z. Lin, H. Hu, B. Chen, S. Lei, J. Tian, and Y. Gao, "Shaped-beam pattern synthesis with sidelobe level minimization via nonuniformly-spaced sub-array," *IEEE Trans. Antennas Propag.*, vol. 70, no. 5, pp. 3421–3436, May 2022, doi: 10.1109/TAP.2022.3143137.

[22] G. Sun, Y. Liu, Z. Chen, S. Liang, A. Wang, and Y. Zhang, "radiation beam pattern synthesis of concentric circular antenna arrays using hybrid approach based on cuckoo search," *IEEE Trans. Antennas Propag.*, vol. 66, no. 9, pp. 4563–4576, Sep. 2018, doi: 10.1109/TAP.2018.2846771.

[23] A. Das, D. Mandal, and R. Kar, "An optimal circular antenna array design considering mutual coupling using heuristic approaches," *Int. J. RF Microw. Comput.-Aided Eng.*, vol. 30, no. 11, p. 114, Nov. 2020, doi: 10.1002/mmce.22391.

[24] A. Das, D. Mandal, and R. Kar, "An optimal circular antenna array design considering the mutual coupling employing ant lion optimization," *Int. J. Microw. Wireless Technol.*, vol. 13, p. 19, Mar. 2020, doi: 10.1017/S1759078720000914.

[25] T. Zheng et al., "IWORMLF: Improved invasive weed optimization with random mutation and Lévy flight for beam pattern optimizations of linear and circular antenna arrays," *IEEE Access*, vol. 8, pp. 19460–19478, 2020, doi: 10.1109/ACCESS.2020.2968476.

[26] Z.-B. Lu, A. Zhang, and X.-Y. Hou, "Pattern synthesis of cylindrical conformal array by the modified particle swarm optimization algorithm," *Prog. Electromagn. Res.*, vol. 79, pp. 415–426, 2008, doi: 10.2528/PIER07103004.

[27] E. Rajo-Iglesias and O. Quevedo-Teruel, "Linear array synthesis using an ant-colony-optimization-based algorithm," *IEEE Antennas Propag. Mag.*, vol. 49, no. 2, p. 70–79, Apr. 2007, doi: 10.1109/MAP.2007.376644.
[28] W.-C. Weng, F. Yang, and A. Z. Elsherbeni, "Linear antenna array synthesis using Taguchi's method: A novel optimization technique in electromagnetics," *IEEE Trans. Antennas Propag.*, vol. 55, no. 3I, pp. 723–730, Mar. 2007, doi: 10.1109/TAP.2007.891548.
[29] J. Li, G. Sun, L. Duan, and Q. Wu, "Multi-objective optimization for UAV swarm-assisted IoT with virtual antenna arrays," *IEEE Trans. Mobile Comput.*, vol. 23, no. 5, pp. 4890–4907, May 2024, doi: 10.1109/TMC.2023.3298888.
[30] G. Sun et al., "Energy efficient collaborative beamforming for reducing sidelobe in wireless sensor networks," *IEEE Trans. Mobile Comput.*, vol. 20, no. 3, pp. 965–982, Mar. 2021, doi: 10.1109/TMC.2019.2955948.
[31] S. Liang et al, "Sidelobe reductions of antenna arrays via an improved chicken swarm optimization approach," *IEEE Access*, vol. 8, pp. 37664–37683, 2020, doi: 10.1109/ACCESS.2020.2976127.
[32] H. Wang, C. Liu, H. Wu, B. Li, and X. Xie, "Optimal pattern synthesis of linear array and broadband design of whip antenna using grasshopper optimization algorithm," *Int. J. Antennas Propag.*, vol. 2020, Jan. 2020, Art. no. 5904018, doi: 10.1155/2020/5904018.
[33] T. Wang, K.-W. Xia, H.-L. Tang, S.-W. Zhang, and M. Sandrine, "A modified wolf pack algorithm for multi constrained sparse linear array synthesis," *Int. J. Antennas Propag.*, vol. 2020, Jan. 2020, Art. no. 9483971, doi: 10.1155/2020/9483971.
[34] A. Das, D. Mandal, S.P. Ghoshal, and R.Kar, "Moth flame optimization based design of linear and circular antenna array for side lobe reduction," *Int. J. Numer. Model., Electron. Netw., Devices Fields*, vol. 32, no. 1, Jan./Feb. 2019, Art. no. e2486, doi: 10.1002/jnm.2486.
[35] K. Guney, A. Durmus, and S. Basbug, "Antenna array synthesis and failure correction using differential search algorithm," *Int. J. Antennas Propag.*, vol. 2014, Mar. 2014, Art. no. 276754, doi: 10.1155/2014/276754.
[36] M. A. Zaman and M. Abdul Matin, "None uniformly spaced linear antenna array design using firefly algorithm," *Int. J. Microw. Sci. Technol.*, vol. 2012, no. 1, 2012, Art. no. 256759, doi: 10.1155/2012/256759.
[37] M. Khodier, "Optimisation of antenna arrays using the cuckoo search algorithm," *IET Microw., Antennas Propag.*, vol. 7, no. 6, pp. 458–464, 2013, doi: 10.1049/iet-map.2012.0692.
[38] K. Guney and A. Durmus, "Pattern nulling of linear antenna arrays using backtracking search optimization algorithm," *Int. J. Antennas Propag.*, vol. 2015, Apr. 2015, Art. no. 713080, doi: 10.1155/2015/713080.
[39] Y. N. Samir, F. W. Zaki, and H. B Nafea, "Performance evaluation of MIMO system in mm wave based on space time block code and different modulation techniques," *Mansoura Eng. J.*, vol. 47, no. 4, pp. 19–28, Aug. 2022, doi: 10.21608/BFEMU.2022.261418.
[40] A. M. Elbir, "CNN-based precoder and combiner design in mmwave MIMO systems," *IEEE Commun. Lett.*, vol. 23, no. 7, pp. 1240–1243, Jul. 2019, doi: 10.1109/LCOMM.2019.2915977.
[41] A. Vizziello, P. Savazzi, K. R. Chowdhury, "A Kalman based hybrid precoding for multi-user millimeter wave MIMO system," *IEEE Access*, vol. 6, pp. 55712–55722, 2018, doi: 10.1109/ACCESS.2018.2872738.
[42] H. Yi, X. Wei, and Y. Tang, "Hybrid precoding based on a switching network in millimeter wave MIMO system," *Electronics*, vol. 11, no. 16, p. 2541, 2022, doi: 10.3390/electronics11162541.
[43] W. Park and J. Choi, "Hybrid precoding and combining strategy for MMSE-based rate balancing in mmWave multiuser MIMO system," *IEEE Access*, vol. 10, pp. 88043–88057, 2022, doi: 10.1109/ACCESS.2022.3199875.
[44] N. M. Tatineni, "Hybrid precoding/combining for single-user and multi-user in mm-wave MIMO system," *Int. J. Innovat. Technol. Explor. Eng.*, vol. 9, no. 2S3, pp. 134–139, 2019.
[45] F. Raisa, Md. R Islam, K. Abdullah, and A. Reza, "Hybrid precoding design using MMSE Baseband precoder for mm-wave multi-user MIMO systems," *Int. J. Recent Technol. Eng.*, vol. 8, no. 2S11, pp. 3486–3486, Sep. 2019, doi: 10.35940/ijrte.B1588.0982S1119.
[46] K. Kaur and V. K. Banga, "Synthesis of linear antenna array using firefly algorithm," *Int. J. Sci. Eng. Res.*, vol. 4, no. 8, pp. 601–606, Aug. 2013.

SAMAR I. FARGHALY received the B.Sc., M.Sc., and Ph.D. degrees in electronics and electrical communications engineering from Tanta University, Egypt, in 2011, 2017, and 2021, respectively, where she has been with the Electronics and Electrical Communications Engineering Department since 2012 and currently works as an Assistant Professor. Her research interests include signal processing and wireless communications (mobile, satellite, MIMO, and radar).

MOSTAFA M. FOUDA (Senior Member, IEEE) received the B.S. degree (as the valedictorian) and the M.S. degree in electrical engineering from Benha University, Egypt, in 2002 and 2007, respectively, and the Ph.D. degree in information sciences from Tohoku University, Japan, in 2011. He is currently an Associate Professor with the Department of Electrical and Computer Engineering, Idaho State University, Pocatello, ID, USA. He is also a Full Professor with Benha University. He was an Assistant Professor with Tohoku University and a Postdoctoral Research Associate with Tennessee Technological University, Cookeville, TN, USA. He has received several research grants, including NSF Japan–U.S. Network Opportunity 3 (JUNO3). He has (co)authored more than 230 technical publications. His current research focuses on cybersecurity, communication networks, signal processing, wireless mobile communications, smart healthcare, smart grids, AI, and IoT. He has guest-edited a number of special issues covering various emerging topics in communications, networking, and health analytics. He is currently serving on the editorial board of IEEE TRANSACTIONS ON VEHICULAR TECHNOLOGY, IEEE INTERNET OF THINGS JOURNAL, and IEEE ACCESS.

MANAL M. EMARA (Member, IEEE) was born in Kafrelsheikh, Egypt, in 1989. She received the B.Sc. degree in electrical power and machines engineering from Kafrelsheikh University, Egypt, in 2011, the M.Sc. degree in electrical power and machines engineering from Tanta University, Egypt, in 2016, and the Ph.D. degree from the School of Electrical Computer Engineering, National Technical University of Athens in 2021. Since 2012, she has been with the Electrical Engineering Department, Kafrelsheikh University, where she currently works as an Assistant Professor. Her research interests are high-voltage engineering and nanodielectric materials. She received the IEEE Caixin Sun and Stan Grzybowski Best Student Paper Award through IEEE ICHVE 2020.